A Section 508–conformant HTML version of this article is available at https://doi.org/10.1289/EHP7058.

Effects of PCB126 on Adipose-to-Muscle Communication in an *in Vitro* Model

Audrey Caron,[1,2] Fozia Ahmed,[1,2] Vian Peshdary,[2,3] Léa Garneau,[1,2] Ella Atlas,[2,3] and Céline Aguer[1,2,4,5]

[1]Institut du Savoir Montfort—recherche, Ottawa, Ontario, Canada
[2]Department of Biochemistry, Microbiology and Immunology, Faculty of Medicine, University of Ottawa, Ottawa, Ontario, Canada
[3]Environmental Health Science and Research Bureau, Health Canada, Ottawa, Ontario, Canada
[4]School of Human Kinetics, Faculty of Health Sciences, University of Ottawa, Ottawa, Ontario, Canada
[5]Interdisciplinary School of Health Sciences, Faculty of Health Sciences, University of Ottawa, Ottawa, Ontario, Canada

Background: Exposure to coplanar polychlorinated biphenyls (PCBs) is linked to the development of insulin resistance. Previous studies suggested PCB126 alters muscle mitochondrial function through an indirect mechanism. Given that PCBs are stored in fat, we hypothesized that PCB126 alters adipokine secretion, which in turn affects muscle metabolism.

Objectives: We determined *a*) the impacts of PCB126 exposure on adipocyte cytokine/adipokine secretion *in vitro*; *b*) whether adipocyte-derived factors alter glucose metabolism and mitochondrial function in myotubes when exposed to PCB126; and *c*) whether preestablished insulin resistance alters the metabolic responses of adipocytes exposed to PCB126 and the communication between adipocytes and myotubes.

Methods: 3T3-L1 adipocytes were exposed to PCB126 (1–100 nM) in two insulin sensitivity conditions [insulin sensitive (IS) and insulin resistant (IR) adipocytes], followed by the measurement of secreted adipokines, mitochondrial function, and insulin-stimulated glucose uptake. Communication between adipocytes and myotubes was reproduced by exposing C2C12 myotubes or mouse primary myotubes to conditioned medium (CM) derived from IS or IR 3T3-L1 adipocytes exposed to PCB126. Mitochondrial function and insulin-stimulated glucose uptake were then determined in myotubes.

Results: IR 3T3-L1 adipocytes treated with PCB126 had significantly higher adipokine (adiponectin, IL-6, MCP-1, TNF-α) secretion and lower mitochondrial function, glucose uptake, and glycolysis. However, PCB126 did not significantly alter these parameters in IS adipocytes. Altered energy metabolism in IR 3T3-L1 adipocytes was linked to lower phosphorylation of AMP-activated protein kinase (p-AMPK) and higher superoxide dismutase 2 levels, an enzyme involved in reactive oxygen species detoxification. Myotubes exposed to the CM from PCB126-treated IR adipocytes had lower glucose uptake, with no alteration in glycolysis or mitochondrial function. Interestingly, p-AMPK levels were higher in myotubes exposed to the CM of PCB126-treated IR adipocytes.

Discussion: Taken together, these data suggest that increased adipokine secretion from IR adipocytes exposed to PCB126 might explain impaired glucose uptake in myotubes. https://doi.org/10.1289/EHP7058

Introduction

Since 1990, the number of individuals with diabetes has quadrupled worldwide, where in 2014, 422 million people were affected by this disease (WHO 2020). Type 2 diabetes accounts for over 90% of diabetes cases (International Diabetes Federation 2020). Type 2 diabetes is caused by insulin resistance in a number of tissues and organs including the liver, adipose tissue, and skeletal muscles, followed by a dysfunction of pancreatic β-cells. The development of insulin resistance is multifactorial, involving the interaction of genes and environmental–behavioral risk factors.

Due to its mass, skeletal muscle is responsible for up to 80% of postprandial glucose disposal (Ferrannini et al. 1985) and it is, therefore, a key player in the development of insulin resistance and type 2 diabetes (Mogensen et al. 2007). Bonnard et al. (2008) showed that insulin resistance was also related to muscle mitochondrial dysfunction, which was caused by oxidative stress in a diet-induced insulin resistant mouse model. In addition, the accumulation of visceral fat is also recognized as a major cause in the development of insulin resistance and type 2 diabetes (Matsuda and Shimomura 2013). As recently reviewed by Longo et al. (2019) hypertrophied adipose tissue leads to increased inflammation and metabolic imbalance. Furthermore, alteration in the secretion of cytokines/adipokines by dysfunctional adipose tissue, including tumor necrosis factor α (TNF-α), leptin, and adiponectin increased oxidative stress and induced mitochondrial dysfunction and insulin resistance in other tissues including skeletal muscle as reviewed by Scherer (2006) and Steinberg (2007). Therefore, altered adipose tissue-derived factors may affect normal adipose-to-muscle communication and thereby lead to the development of insulin resistance and type 2 diabetes.

It has been recently hypothesized that exposure to environmental pollutants may explain the sharp increase in the prevalence of type 2 diabetes (Pizzorno 2016). Epidemiological studies found a correlation between exposure to various persistent organic pollutants, such as polychlorinated biphenyls (PCBs) and *p*,*p*-dichlorodiphenylchloroethane (DDT), the development of insulin resistance and type 2 diabetes (Everett et al. 2007; and reviewed by Neel and Sargis 2011, Sargis 2014). PCBs are very stable compounds that accumulate in adipose tissue due to their lipophilicity. The phenyl rings and chlorine substituents arrangements dictate the PCB mechanism of action. Dioxin-like PCBs (coplanar), such as PCB77 and PCB126, were associated with a wide range of toxic effects, such as reproductive dysfunction, immunotoxicity, liver damage, metabolic dysregulation, and developmental defects (WHO 2010). Their toxicity is mainly mediated through the activation of the aryl hydrocarbon receptor (AhR) (Davis and Safe 1990). As reviewed by Giesy and Kurunthachalam (2002), non-dioxin–like PCB exposure in rodents was also associated with liver damage and developmental and neurological effects, but their toxicity is not via AhR activity. Exposure to PCBs most commonly found in the environment—PCB77, 118, 126, and 153, or mixtures of PCBs (e.g., Aroclor 1254)—resulted in the development of insulin resistance and glucose intolerance in rodents (Gray et al. 2013; Ruzzin et al. 2010; Zhang et al. 2015). Furthermore, coplanar PCB exposure was linked to mitochondrial dysfunction and inflammation in mice (Ruzzin et al. 2010), as well as in adipocytes (Baker et al. 2013) and human umbilical vascular

Address correspondence to Céline Aguer, Institut du Savoir Montfort, 1E103, 713 Montreal Rd., Ottawa ON K1K 0T2 Canada. Telephone: (613) 746 4621. Email: celineaguer@montfort.on.ca

Supplemental Material is available online (https://doi.org/10.1289/EHP7058).

The authors declare they have no actual or potential competing financial interests.

Received 11 March 2020; Revised 27 August 2020; Accepted 8 September 2020; Published 7 October 2020.

Table 1. Composition of adipocyte (3T3-L1) differentiation media.

Adipocyte insulin sensitivity status	ADM1	ADM2	ADM3
IS adipocytes	DMEM low glucose (1 g/L), 10% FBS, 0.5 mM IBMX, 1 µM dexamethasone, 1× AA, 100 nM insulin	DMEM low glucose (1 g/L), 10% FBS, 1× AA, 100 nM insulin	DMEM low glucose (1 g/L), 10% FBS, 1× AA
IR adipocytes	DMEM low glucose (1 g/L), 10% FBS, 0.5 mM IBMX, 1 µM dexamethasone, 1× AA, 500 nM insulin	DMEM low glucose (1 g/L), 10% FBS, 1× AA, 500 nM insulin	

Note: AA, antimycotic–antibiotic; ADM, adipocyte differentiation medium; DMEM, Dulbecco's Modified Eagle Medium; IBMX, 3-isobutyl-1-methylxanthine; IR, insulin resistant; IS, insulin sensitive.

endothelial cells (Wang et al. 2010). Moreover, diet-induced insulin resistance, adiposity, and adipose tissue inflammation in mice was exacerbated by pollutants (Gray et al. 2013).

Despite the growing body of evidence supporting the role of coplanar PCBs in the development of insulin resistance and type 2 diabetes, the effects of PCB exposure on the insulin sensitivity and energy metabolism of skeletal muscle has not been thoroughly investigated. Our group demonstrated that L6 skeletal muscle cells exposed for 24 h to PCB126 had 20% lower glucose uptake and glycolysis than vehicle-treated cells (Mauger et al. 2016). This altered glucose metabolism in PCB126-treated L6 myotubes was consistent with another study showing decreased glucose transporter 4 (GLUT4) translocation and glucose uptake in muscle of rats exposed to a mixture of PCBs (Williams et al. 2013). Furthermore, we recently demonstrated that rats exposed acutely to PCB126 had lower mitochondrial function measured in permeabilized muscle fibers that was associated with an alteration in the expression levels of a number of enzymes involved in reactive oxygen species (ROS) detoxification (Tremblay-Laganière et al. 2019). However, no mitochondrial dysfunction was detected *in vitro* in L6 muscle cells exposed directly to PCB126 (Mauger et al. 2016). Skeletal muscle response to PCB126 was therefore different *in vivo* (whole organism) and *in vitro* (direct exposure of muscle cells to PCB126). Taken together, these studies suggest that the development of mitochondrial dysfunction in the skeletal muscle of rats exposed to PCB126 was not the result of a direct effect of the pollutant on muscle mitochondria.

Because of their lipophilic properties, PCBs accumulate mostly in adipose tissue (Beyer and Biziuk 2009; Imbeault et al. 2002; Kodavanti et al. 1998; Matthews and Dedrick 1984). Therefore, we hypothesized that PCB126 might first induce adipose tissue dysfunction, resulting in altered adipokine and inflammatory cytokine secretion, which in turn could induce mitochondrial dysfunction in skeletal muscle. The overall aim of the present study was thus to study the role of adipose-to-muscle communication in PCB126-induced metabolic defects using an *in vitro* model. The specific objectives were *a*) to determine the effect of PCB126 exposure on adipocyte cytokine/adipokine production *in vitro*; *b*) to test whether the communication between adipose tissue and muscle explains both abnormal muscle glucose metabolism and muscle mitochondrial dysfunction when exposed to PCB126; and *c*) to determine whether insulin resistance in adipocytes alters their responses to PCB126 and alters the communication between adipocytes and muscle cells.

Methods

Cell Culture

All cell lines were cultured in a humidified incubator [Thermo Scientific Forma Steri-Cycle™ carbon dioxide (CO_2) incubator] at 37°C with 5% CO_2.

3T3-L1 Adipocytes

3T3-L1 (ATCC® CL-173™) were grown in low-glucose Dulbecco's Modified Eagle Medium (DMEM) (1.0 g/L glucose, 4 mM L-glutamine and 110 mg/L sodium pyruvate; Wisent), 10% calf serum (Wisent), and 1× antimycotic–antibiotic (AA; Wisent). The medium was changed every 2 d until cells reached approximately 90% confluence. 3T3-L1 cells were then differentiated into adipocytes for 10 d using three different adipocyte differentiation media (ADM1, ADM2, and ADM3) (Table 1) at specific times as described in Figure 1. Insulin resistance (IR) was induced by using differentiation media with high concentrations of insulin (500 nM; Sigma-Aldrich; see Table 1 for details). For insulin sensitive (IS) adipocytes, the concentration of insulin in ADM1 and ADM2 was 100 nM and no insulin was present in ADM3 (Table 1).

C2C12 Muscle Cells

C2C12 myoblasts (Sigma-Aldrich) were grown in low-glucose DMEM, 10% fetal bovine serum (FBS; Wisent), and 1× AA. The medium was refreshed every other day until cells reached approximately 90% confluence. C2C12 cells were then differentiated into myotubes for 7 d in low-glucose DMEM, 2% FBS, and 1× AA. Differentiation medium was refreshed every 2 or 3 d.

Mouse Primary Muscle Cells

Mouse primary myoblasts derived from gastrocnemius and tibialis muscles of wild-type mice with a C57BL/6J background were a kind gift from M. Foretz (Institut Cochin, Paris, France). Mouse primary muscle cells were cultured on Matrigel® (1× in DMEM; Corning)-coated equipment in a DMEM:F12 1:1 medium (Wisent), supplemented with 20% FBS, 1× AA, 3 µg/mL gentamicin (Wisent), and 5 ng/mL recombinant mouse fibroblast growth factor basic (ThermoFisher). At approximately 90% confluence, mouse primary muscle cells were differentiated into myotubes for 7 d in low-glucose DMEM supplemented with 2% FBS, 1× AA, and 3 µg/mL gentamicin. Differentiation medium was refreshed every 2 or 3 d.

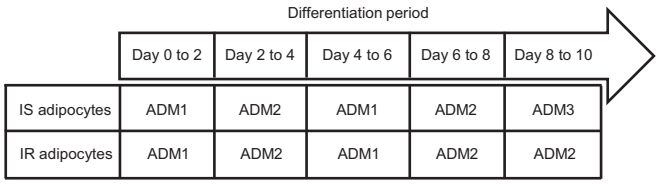

Figure 1. Detailed differentiation protocol of 3T3-L1 adipocytes. 3T3-L1 cells were differentiated for a total period of 10 d using different adipocyte differentiation media (ADM) as described in the figure. The composition of each ADM is described in detail in Table 1. Note: IR, insulin resistant; IS, insulin sensitive.

Table 2. Primer sequence used for quantitative reverse transcription polymerase chain reaction (RT-qPCR).

Target Gene	Primer sequence
Il-6	Forward: 5′-GCCTTCTTGGGACTGATGCT-3′
	Reverse: 5′-TGCCATTGCACAACTCTTTTC-3′
Adiponectin	Forward: 5′-TGACGACACCAAAAGGGCTC-3′
	Reverse: 5′-CACAAGTTCCCTTGGGTGGA-3′
Cyp1a1	Forward: 5′-CATTTGAGAAGGGCCACATCC-3′
	Reverse: 5′-TGTGTCAAACCCAGCTCCAA-3′
β-actin	Forward: 5′-GACTTCGAGCAAGAGATGGC-3′
	Reverse: 5′-CCAGACAGCACTGTCTTGGC-3′

PCB126 Treatments

Treatments were done once the adipocytes were fully differentiated to study the impact of PCB126 on the secretome and metabolism of mature adipocytes. On Day 10 of differentiation, adipocytes were exposed to 0, 1, 10, or 100 nM of PCB126 (ULTRA Scientific) dissolved in 0.1% dimethyl sulfoxide (DMSO; Sigma-Aldrich) for 24 h. These concentrations were chosen to represent environmentally relevant PCB126 concentrations. In fact, exposure to PCB126 in Canadian Inuit population was measured to be between 0.05 nM and 27 nM (Singh and Chan 2017), whereas the daily intake of PCB126 was estimated to be 12 pg/d (U.S. EPA 2003). Untreated cells (0 nM PCB126) were exposed to 0.1% DMSO (vehicle). In order to determine whether some factors secreted by adipocytes upon exposure to PCB126 altered the metabolism of myotubes, after the 24-h PCB126 treatment, the conditioned medium (CM) of adipocytes was used to treat differentiated C2C12 myotubes or mouse primary myotubes for 24 h. This model was chosen over the coculture model to study the unidirectional communication from adipocytes to myotubes. As a control condition, differentiated myotubes were also treated with the same concentrations of PCB126 in ADM2 (IR) or ADM3 (IS) for 24 h (direct exposure). After the 24-h treatments, cells were prepared for the different experiments described below.

Cell Viability

To determine whether the different treatments affected cell survival, viability was measured using the PrestoBlue® method (ThermoFisher) according to manufacturer's instructions. 3T3-L1 and C2C12 cells were grown and differentiated in 96-well plates (20,000 cells/well) and treated with PCB126 or 3T3-L1 CM for 24 h as described above. Cells were then incubated for 30 min in 1 × PrestoBlue® reagent and absorbance was measured at 570 nm and 600 nm (reference wavelength) (Synergy™ HT multi-mode microplate reader; BioTek instruments). Each experiment was done in triplicate for 3T3-L1 adipocytes and in six replicates for C2C12 myotubes, and repeated on three independent cultures ($n = 3$).

Lipid Accumulation

To determine whether PCB126 treatments or IS and IR conditions had an effect on 3T3-L1 and C2C12 intracellular lipid accumulation, lipid droplets were stained by Oil Red O (Sigma-Aldrich). Lipid accumulation is an indicator of adipocyte differentiation. In muscle cells, intramyocellular lipid accumulation is believed to be related to insulin resistance development (Aguer et al. 2010; Krssak et al. 1999; Perseghin et al. 1999). For these experiments, 3T3-L1 cells were grown and differentiated in 6-well plates, whereas C2C12 cells were grown and differentiated in 12-well plates. The cells were treated with PCB126 or 3T3-L1 CM as described above, and then fixed with 4% paraformaldehyde (Alfa Aesar) in phosphate-buffered saline for 10 min. Lipid droplets were stained with 0.5% Oil Red O dissolved in chloroform:ethanol (1:1; Fisher Scientific) for 10 min, as previously described (Aguer et al. 2010). Cells were washed three times with distilled water and visualized by light microscope (EVOS XL Core Imaging System) using a 40 × objective and a constant light intensity. Oil Red O was then extracted with 70% isopropanol (Fisher Scientific) and absorbance read at 490 nm (Aguer et al. 2010). Each experiment was done in duplicate and repeated on three independent cell cultures ($n = 3$).

mRNA Quantification by Quantitative Reverse Transcription Polymerase Chain Reaction (RT-qPCR)

3T3-L1 cells were grown and differentiated in six-well plates followed by 24-h treatment with PCB126, as described above. Cells were then lysed using RNease lysis buffer with 1% mercaptoethanol (Sigma-Aldrich) from the RNeasy Mini Kit (Qiagen) and lysates were stored at –80°C. Total RNA was extracted from cell lysates using the RNase Mini Kit where genomic DNA was removed using the RNase-Free DNase Kit (Qiagen) following the manufacturer's recommendations. RNA concentration and extraction quality were measured using a NanoDrop™ 1000 Spectrophotometer (ThermoFisher). Then, 0.5 µg RNA was reverse transcribed with iScript Complementary DNA (cDNA) Synthesis Kit (Bio-Rad) following the manufacturer's protocol in a CFX96-polymerase chain reaction (PCR) Detection System (Bio-Rad). cDNA was amplified and quantified in a CFX96-PCR Detection System using the iQSYBR SsoFast EvaGreen Supermix (Bio-Rad). Primers for each target genes are summarized in Table 2. All genes were normalized to β-actin levels and analyzed using the comparative cycle threshold (C_T) (ΔΔCT) method, as previously described (Schmittgen and Livak 2008). Each independent experiment ($n = 3$) was done in triplicate.

Adipokine Measurements

To determine whether the different treatments affected cytokine and adipokine secretion, 3T3-L1 cells were grown and differentiated in 6-well plates followed by 24-h treatments as described above. At the end of the treatments, culture media were collected and stored at –80°C until further cytokine/adipokine measurements. Cells were lysed in 0.05 M sodium hydroxide (NaOH; Fisher Scientific) and protein quantified using the Bradford method (Bio-Rad). Cytokine/adipokine [interleukin-6 (IL-6), TNF-α, leptin, adiponectin, monocyte chemoattractant protein-1 (MCP-1), plasminogen activator inhibitor-1 (PAI-1), and resistin] concentrations in the different culture media were determined by the Bio-Plex method using the mouse adipocyte magnetic bead panel kit (MADCYMAG-72K-07; Millipore), according to manufacturer's instructions (EMD Millipore 2013). Samples were diluted 20 × in DMEM low glucose and 10 µL of each sample and standards were added to the detection beads and stirred rapidly at room temperature for 2 h, washed three times followed by addition of secondary antibodies coupled to biotin for 30 min. After three washes, streptavidin–phycoerythrin conjugate was added to each well for 10 min at room temperature, rinsed three times, and read by the Bio-Plex (Bio-Plex MAGPIX Multiplex Reader; Bio-Rad). Each experiment was done in duplicate and repeated with media from three independent experiments ($n = 3$).

Adipokines measured with the Bioplex method are expressed relative to the vehicle condition because experiments were done independently for IS and IR conditions (preparation of samples and Bioplex experiments done at different times). In order to compare IS and IR conditions, and to confirm the Bioplex results, some adipokines were also remeasured, using enzyme-linked immunosorbent assay (ELISA) kits, in the CM of adipocytes prepared in parallel for IS and IR conditions. Levels of adiponectin in the CM were determined after a 1:1,000 dilution using the adiponectin mouse ELISA kit (EKL54022; Biomatik). Levels of IL-

6 were measured after a 1:2 CM dilution using the IL-6 mouse ELISA kit (BMS603-2; Thermo-Fisher). Levels of leptin and TNF-α were determined in undiluted samples using the leptin mouse ELISA kit (EKB01861; Biomatik) and the TNF-α mouse ELISA kit (EKA51917; Biomatik), respectively. Each measurement was done in duplicate and repeated with media from three or four independent experiments ($n = 3$–4).

Lipolysis

To determine whether PCB126 or insulin sensitivity status in adipocytes had an impact on lipolysis, glycerol and free fatty acids (FFAs) were quantified in the adipocyte media by using a lipolysis quantification kit (LIP-3-NC-L1; ZenBIO) following the manufacturer's protocol. Briefly, 3T3-L1 adipocytes were differentiated and treated with PCB126 as described above, in 96-well plates (20,000 cells/well). Then, they were incubated for 3 h in assay buffer with PCB126. The media was used to quantify FFA and glycerol secretion. Absorbance was read at 540 nm. Each experiment was done in triplicate and repeated with media from three independent experiments ($n = 3$).

Mitochondrial Respiration and Glycolysis

3T3-L1 and C2C12 energy metabolism—mitochondrial function and glycolysis—were measured by determination of oxygen consumption rates (OCRs) and of extracellular acidification rates (ECARs), respectively, using an extracellular flux analyzer (Seahorse XFe96; Agilent). The protocol provided by Seahorse Bioscience was followed for these experiments with slight modifications. At the end of the 24-h treatments, cells were rinsed three times with assay buffer (8.3 g/L DMEM, 2 mM sodium pyruvate, 5 mM dextrose, and 0.75 mM L-glutamine, pH 7.4; all from Sigma-Aldrich). Cells were then incubated at 37°C, without CO_2, in 180 µL of assay buffer for 45 min. OCR and ECAR were first measured at baseline for four cycles including: a 2-min measurement, medium mixing for 2 min, and a 2-min pause before starting the next cycle. Then, inhibitors of the respiratory chain were injected into each well in the following order: oligomycin, carbonyl cyanide-4-(trifluoromethoxy)phenylhydrazone (FCCP), and antimycin A (all from Sigma-Aldrich). After each injection, OCR and ECAR were measured for three cycles (measuring, mixing, rest; 2 min each). Final inhibitor concentrations used were 600 ng/mL oligomycin, 1 µM FCCP, and 2 µM antimycin A for 3T3-L1 and 600 ng/mL oligomycin, 1 µM FCCP, and 4 µM antimycin for C2C12. At the end of the experiment, cells were lysed in 50 µL of 0.05 M NaOH and proteins were quantified by the Bradford method. Mitochondrial OCR [non-mitochondrial OCR (antimycin A condition) subtracted from total OCR] and ECAR values are expressed per microgram of total cellular proteins. Each experiment was done in five or six replicates and repeated on four independent cultures ($n = 4$).

Glucose Uptake

3T3-L1, C2C12, and mouse primary muscle cells were grown and differentiated in 24-well plates (100,000 cells/well) or 48-well plates (50,000 cells/well), followed by 24-h treatments, as described above. Glucose uptake was measured as described by Klip et al. (1984). After PCB126 treatment, cells were starved for 3 h in serum-free DMEM. During the last 20 min of the starvation period, 100 nM insulin was added in half of the wells. Cells were then washed and incubated in 4-(2-hydroxyethyl)-1-piperazineethanesulfonic acid (HEPES) buffered saline [140 mM sodium chloride (NaCl; Fisher Scientific), 20 mM HEPES-Na (Sigma-Aldrich), 5 mM potassium chloride (Fisher Scientific), 2.5 mM magnesium sulfate; Fisher Scientific), and 1 mM calcium chloride (Sigma-Aldrich); pH 7.4] with 10 µM 2-deoxy-glucose (Sigma-Aldrich) and 0.5 µCi/mL ^{3}H-2-deoxy-glucose(Perkin Elmer). Cytocholasin B (5 µM; Sigma-Aldrich) was used to determine nonspecific glucose uptake. Cells were lysed in 0.5 mL of 0.05 M NaOH and 0.4 mL were measured by scintillation counting with a Tri-Carb2910TR counter (Perkin Elmer). The remaining cell lysate was used to determine protein content using a Bradford protein assay. Each experiment was done in triplicate and repeated on three or four independent cultures ($n = 3$–4).

Western Blots

3T3-L1 adipocytes and C2C12 myotubes were lysed in lysis buffer (20 mM Tris-hydrochloride, 50 nM NaCl, 250 mM sucrose, 1% 100× Triton™, 50 mM sodium fluoride, 5 mM sodium pyrophosphate, 1 mM sodium orthovanadate). Twenty to 30 µg of proteins were separated by sodium dodecyl sulfate polyacrylamide gel electrophoresis and then transferred to nitrocellulose membranes (GE Healthcare). Monoclonal anti-glutathione peroxidase 1 (anti-GPx1; ab108427), monoclonal anti-GPx4 (ab125066), polyclonal anti-glutaredoxin 2 (anti-Grx2; ab191292), MitoProfile® Total OXPHOS Rodent WB Antibody Cocktail (anti-ATP5a, anti-complex III, anti-complex II; MS604) (all from Abcam), monoclonal anti-catalase (D5N7V; #14097), polyclonal anti-α-tubulin (#2144), monoclonal glyceraldehyde-3-phosphate dehydrogenase (14C10), monoclonal anti-AS160 [protein kinase B (Akt) substrate of 160 kDa; C6947; #2670S], polyclonal antiphospho-AS160 (Thr 642; #4288S), polyclonal anti-phospho-insulin receptor substrate 1 (anti-p-IRS1; S307; #2381S), polyclonal anti-phospho-Akt (S473; #9271S), monoclonal anti-Akt (C67E7; #4691S), polyclonal 3α/β (GSK3; S2119; #9331S), polyclonal anti-phospho-AMP-activated protein kinase (p-AMPK; #2535S), polyclonal anti-AMPK (#2532S) (all from Cell Signaling Technology), and polyclonal anti-superoxide dismutase (SOD2) (sc-30080, Santa Cruz), were used as primary antibodies at a dilution of 1:1000. The secondary antibodies used were anti-mouse (sc-516102) and anti-rabbit (sc-2357) antibodies coupled to horseradish peroxidase (Santa Cruz), diluted 1:5,000. Proteins were visualized using SuperSignal West Pico Western Blot Kit (34580; Thermo Scientific) or Clarity Western enhanced chemiluminescence Substrate (170-5061; Bio-Rad) and imaged using a ChemiDoc™ Imager and VisionWorks LS (Ultra-Violet Products Ltd., UVP™). Expression of proteins was quantified by densitometry analysis using ImageJ program (Schneider et al. 2012).

Statistical Analysis

Data shown are the means ± standard error of the mean (SEM) of at least three independent experiments. First, the average of the technical replicates within each independent experiment was determined, and then the mean of the three to four independent experiments were calculated. The SEM presented on the figures represents the SEM of the independent experiments. A Student's *t*-test or one- or two-way analysis of variance (ANOVA) with Fisher's protected least significant difference (PLSD) post hoc test were used to determine statistical differences using Statview software (version 5.0; SAS Institute) and GraphPad Prism (version 6.0e; GraphPad). With the Fisher's PLSD post hoc test used, we compared only PCB126-treated cells to the vehicle (0 nM PCB, 0.1% DMSO). A $p < 0.05$ was considered significant.

Results

Effect of Insulin Concentrations on Insulin Sensitivity and Lipid Accumulation in Differentiating 3T3-L1 Adipocytes

In order to induce insulin resistance in 3T3-L1 adipocytes, 3T3-L1 cells were exposed to high concentrations of insulin (500 nM)

during differentiation (IR condition). Insulin-stimulated glucose uptake was significantly higher in 3T3-L1 adipocytes in the IS condition than in the IR condition (Figure S1A, fold increase in response to insulin: $p = 0.0438$ IS vs. IR). Moreover, there was no difference in lipid accumulation between IS and IR 3T3-L1 adipocytes in basal conditions (no acute insulin treatment), suggesting that the two differentiation protocols did not affect adipogenesis (Figure S1B).

Effect of Direct and Indirect PCB126 Exposure on Lipid Accumulation and Cell Viability in IS and IR Adipocytes and C2C12 Myotubes

We determined the effect of PCB126 or CM treatments on neutral lipid accumulation and cell viability in IS and IR 3T3-L1 adipocytes and C2C12 myotubes. As shown in Figure S2, neither PCB126/CM treatments nor IS or IR conditions significantly altered intracellular lipid accumulation (Figure S2A) and cell viability (Figure S2B) in 3T3-L1 adipocytes and C2C12 myotubes.

Effect of Direct and Indirect PCB126 Exposure on Cyp1a1 mRNA Expression in IS and IR Adipocytes and C2C12 Myotubes

3T3-L1 adipocytes exposed to 100 nM PCB126 for 24 h had a 35-fold and a 85-fold higher expression of the gene for cytochrome P450 family 1 subfamily A member 1 (*Cyp1a1*) mRNA in IS and IR conditions, respectively, compared with vehicle-treated cells ($p = 0.0026$; Figure 2A). No significant differences in *Cyp1a1* expression levels were observed in the IS vs. IR conditions (Figure 2A). Direct exposure of C2C12 to PCB126 or exposure of C2C12 to CM from PCB126-treated adipocytes at the highest concentrations (10 and 100 nM) also resulted in higher *Cyp1a1* mRNA, but it did not reach statistical significance (Figure S3).

Adipocytokine Expression and Secretion by Adipocytes in Response to PCB126 Treatment in IS and IR Conditions

We then determined whether a 24-h PCB126 exposure altered the cytokine profile in IS and IR 3T3-L1 adipocytes by assessing

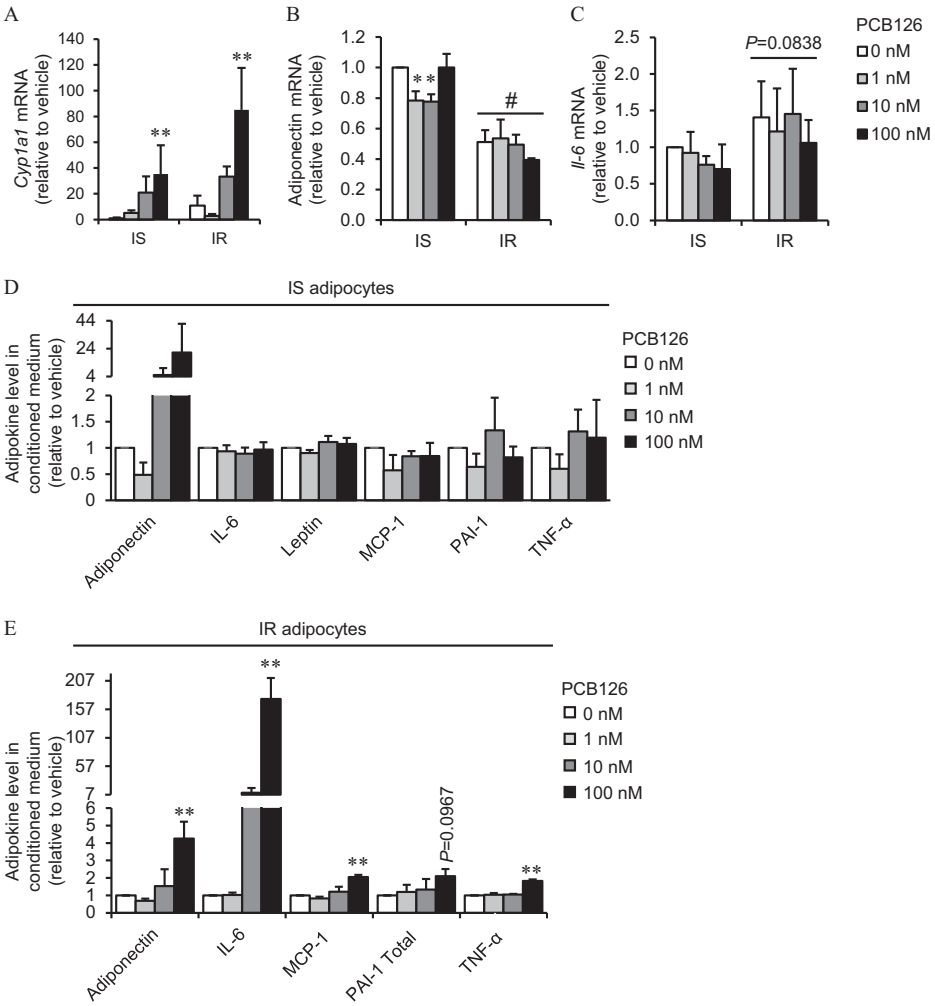

Figure 2. Effect of PCB126 exposure and insulin sensitivity conditions on adipokine expression and secretion in 3T3-L1 adipocytes. 3T3-L1 adipocytes were differentiated in insulin sensitive (IS) and insulin resistant (IR) conditions and treated for the last 24 h of differentiation with different PCB126 concentrations. (A–C) *Cyp1a1* (A), adiponectin (B), and *Il-6* (C) mRNA levels normalized to β-actin mRNA levels and analyzed using the comparative cycle threshold (C_T) ΔΔCT method. Average of normalized ΔΔCT is presented relative to the vehicle (IS, no PCB) ± SEM. $n = 3$ independent experiments, each independent experiment was done at least in triplicate. *, $p < 0.05$ and **, $p < 0.01$ compared with 0 nM PCB126; #, $p < 0.05$ compared with IS adipocytes (two-way ANOVA with Fisher's PLSD post hoc test). (D,E) Adipokines secreted in the medium of 3T3-L1 adipocytes differentiated in IS (D) or IR (E) conditions. Data are presented relative to the vehicle as mean ± SEM. $n = 3$ independent experiments, each independent experiment was done in two replicates. **, $p < 0.01$ compared with 0 nM PCB126 (one-way ANOVA with Fisher's PLSD post hoc test). The exact mean and SEM values for data presented here can be found in Tables S1–S5. Note: ANOVA, analysis of variance; PLSD, protected least significant difference; SEM, standard error of the mean.

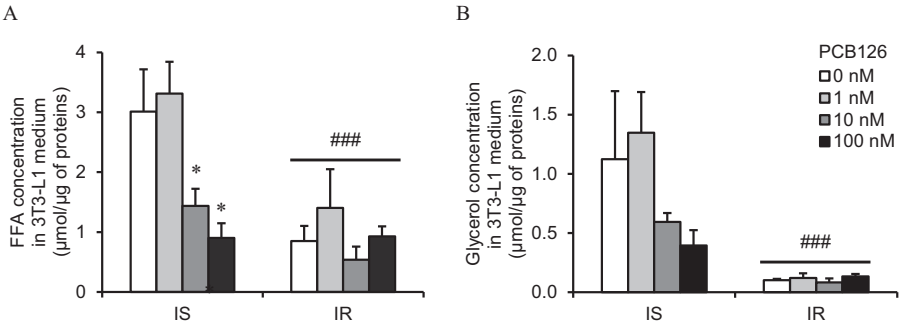

Figure 3. Effect of PCB126 exposure and insulin sensitivity conditions on lipolysis in 3T3-L1 adipocytes. 3T3-L1 adipocytes were differentiated in insulin sensitive (IS) and insulin resistant (IR) conditions and treated for the last 24 h of differentiation with different PCB126 concentrations. As markers of lipolysis, free fatty acid (FFA) (A) and glycerol (B) levels were measured in the conditioned medium as described in the "Methods" section. Data are presented as mean ± SEM. $n = 3$ independent experiments, each independent experiment was done in two replicates. *, $p < 0.05$ compared with 0 nM PCB126; ###, $p < 0.001$ main effect of IR conditions (two-way ANOVA with Fisher's PLSD post hoc test). The exact mean and SEM values for data presented here can be found in Tables S6 and S7. Note: ANOVA, analysis of variance; PLSD, protected least significant difference; SEM, standard error of the mean.

mRNA expression and secretion of cytokines/adipokines. IS adipocytes treated with 1 and 10 nM PCB126 had significantly lower expression of adiponectin mRNA compared with vehicle-treated cells ($p = 0.0492$ and 0.0397, respectively; Figure 2B). In IR adipocytes, PCB126 treatment did not significantly alter adiponectin mRNA expression, but adiponectin mRNA expression was significantly lower in IR compared with IS adipocytes, independent of PCB126 treatment (IR effect: $p = 0.0003$; Figure 2B). *Il-6* mRNA expression was similar in PCB126-exposed IS and IR adipocytes (Figure 2C), although it trended higher in IR adipocytes compared with IS adipocytes; however, it did not reach statistical significance (IR effect: $p = 0.0838$; Figure 2C). In addition, in IS adipocytes, PCB126 treatment did not significantly alter the secretion of cytokines/adipokines (Figure 2D). However, compared with vehicle-treated cells, IR adipocytes treated with 100 nM PCB126 did have a significantly higher secretion of adiponectin ($p = 0.0098$), IL-6 ($p = 0.0002$), MCP-1 ($p = 0.0018$), and TNF-α ($p < 0.0001$) and tended to have higher secretion of PAI-1 ($p = 0.0967$) (Figure 2E). Leptin was not detected in the CM of IR adipocytes treated with 0, 1, or 10 nM PCB126, whereas it was detected when IR adipocytes were treated with 100 nM PCB126, suggesting higher leptin secretion when exposed to 100 nM PCB126 (Figure S4A). Resistin was also measured in the CM of IS and IR adipocytes, but it was not detected with the kit used. In this first set of experiments, IS and IR adipocytes were not prepared at the same time, preventing the comparison between the two differentiation conditions. In order to compare adipokine secretion between IS and IR conditions, and to confirm results obtained with the Bioplex method, some adipokines were also measured by ELISA kits. IL-6 levels were significantly higher in the medium of IR adipocytes compared with IS adipocytes, independent of PCB126 treatments (IR effect: $p = 0.0062$; Figure S4B). Both IS and IR adipocytes had significantly higher secretion of IL-6 after exposure to 100 nM PCB126 (PCB126 effect: $p = 0.0313$). Adiponectin levels were higher in the medium of IR compared with IS adipocytes, independent of PCB126 treatments (IR effect: $p < 0.001$), whereas adiponectin levels in the medium of both IS and IR adipocytes were significantly higher after exposure to 10 nM PCB126 compared with vehicle-treated cells (PCB126 effect: $p = 0.0093$; Figure S4C). Leptin levels were not significantly different between IS and IR conditions, and PCB126 treatments did not alter leptin levels in the medium of either IS or IR adipocytes (Figure S4D). This result does not confirm the higher leptin secretion in the medium of IR adipocytes measured with the Bioplex method. It is, however, important to note that leptin levels measured in the medium of adipocytes was very low and close to the detection level of the ELISA kit used, which can explain the absence of measured effects. TNF-α was also measured in the medium of adipocytes but was not detected with the ELISA kit used.

Effect of PCB126 Treatment and Insulin Resistance on Lipolysis

We then determined whether a 24-h PCB126 exposure or insulin resistant conditions altered the rate of lipolysis in 3T3-L1 adipocytes as measured by FFA and glycerol secretion. IS adipocytes exposed to 10 and 100 nM PCB126 for 24 h had lower lipolytic rates compared with the vehicle condition (for FFA concentration: $p = 0.049$ and $p = 0.0147$ for 10 and 100 nM PCB126, respectively) (Figure 3A). However, in IR adipocytes, a 24-h PCB126 treatment did not significantly alter the lipolytic rate (Figure 3). In addition, IR adipocytes had a significantly lower lipolytic rate than IS adipocytes (IR effect: $p = 0.0009$ and $p = 0.0005$ for FFA concentration and glycerol concentration, respectively) (Figure 3).

Effect of Direct or Indirect PCB126 Exposure on Mitochondrial Function in IS and IR Adipocytes and Myotubes

Mitochondrial function in IS and IR adipocytes directly treated with PCB126. We first determined the effect of a 24-h exposure to PCB126 in IS and IR conditions on adipocyte mitochondrial function. In IS adipocytes, OCR was not altered by a 24-h PCB126 exposure (Figure 4A), whereas IR adipocytes treated with 1 or 10 nM PCB126 had significantly lower OCRs and proton leak (state 4) OCRs (Figure 4B) (for 1 nM $p = 0.0279$ and 0.0429 and for 10 nM $p = 0.0480$ and 0.0448 for resting and proton leak OCR, respectively). To determine if this altered mitochondrial function in IR adipocytes exposed to PCB126 was the result of lower levels of mitochondrial complexes, we measured the impact of PCB126 on the expression of the respiratory chain complexes (Figure 4C,D). IR adipocytes treated with 100 nM PCB126 showed significantly higher ATP5A expression compared with vehicle-treated cells ($p = 0.0065$). A slightly higher ATP5A protein expression was also seen at 10 nM ($p = 0.0607$). There was also a tendency for higher expression of complexes II and III with 24-h PCB126 exposure in IR adipocytes, without reaching significance.

Mitochondrial function in C2C12 myotubes directly treated with PCB126 or treated with the CM of PCB126-treated adipocytes. We then determined whether exposure to CM from 3T3-L1 adipocytes exposed to PCB126 altered mitochondrial

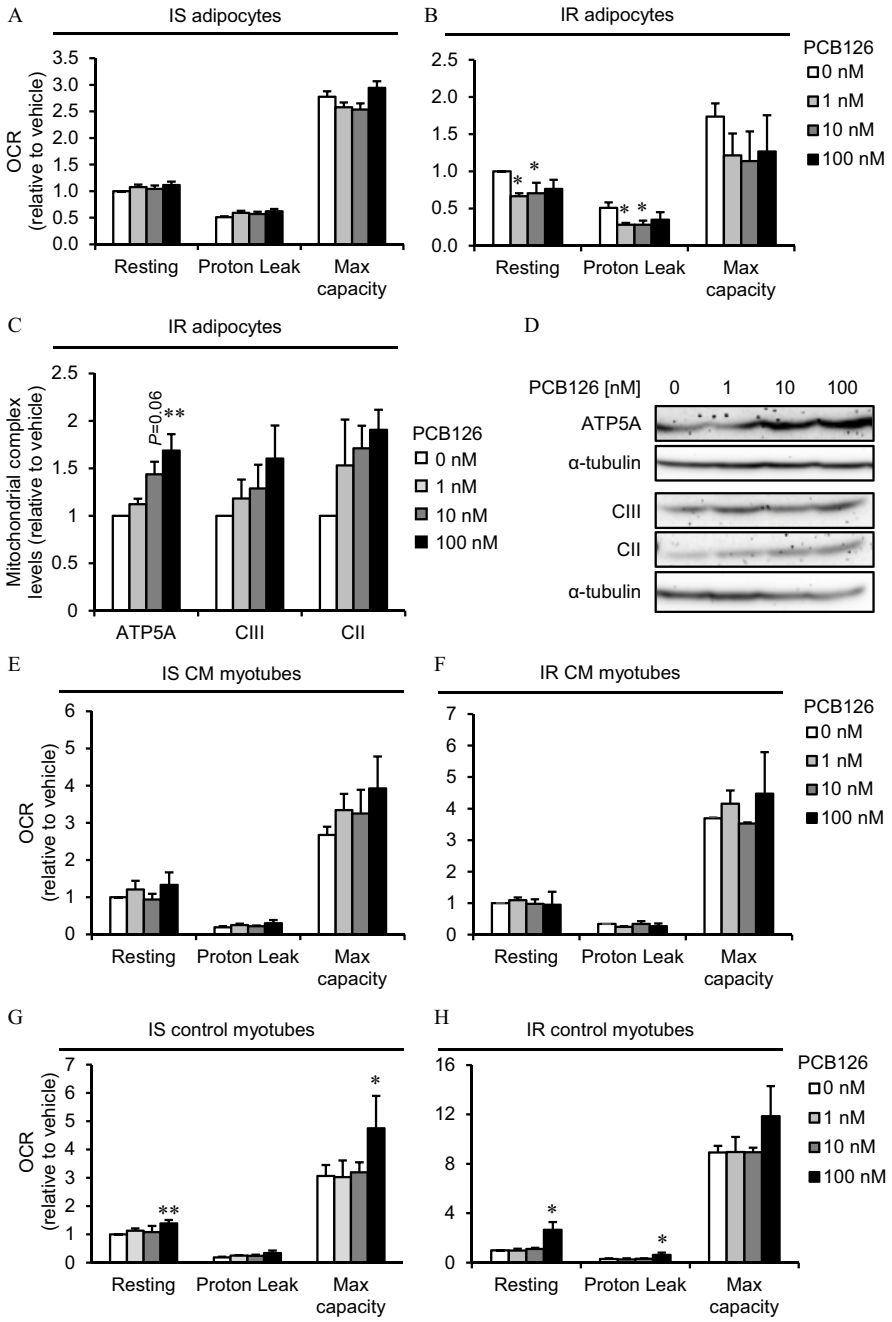

Figure 4. Mitochondrial function in 3T3-L1 adipocytes exposed to PCB126 in different insulin sensitivity conditions and in C2C12 myotubes exposed to the conditioned medium (CM) of insulin sensitive (IS) and insulin resistant (IR) adipocytes treated with PCB126. (A,B) 3T3-L1 adipocytes were differentiated in IS (A) and IR (B) conditions and treated for the last 24 h of differentiation with different PCB126 concentrations. (C,D) Levels of mitochondrial complexes (complexes II and III and ATPase) in 3T3-L1 adipocytes differentiated in IR conditions and exposed for 24 h to different concentrations of PCB126. (C) Quantification by density analysis; (D) representative Western blots. α-Tubulin was used as a loading control. $n = 3$ independent experiments. (E,F) Differentiated C2C12 myotubes were exposed for the last 24 h of differentiation to the CM of 3T3-L1 adipocytes exposed to different PCB126 concentrations in IS (E) or IR conditions (F). (G,H) Differentiated C2C12 myotubes were directly exposed for the last 24 h of differentiation to different PCB126 concentrations in IS (G) or IR conditions (H). Oxygen consumption rates (OCRs) were measured with a Seahorse analyzer (Agilent). OCRs were first measured in resting conditions, and cells were treated subsequently with 600 ng/mL oligomycin, 1 μM carbonyl cyanide-4-(trifluoromethoxy)phenylhydrazone (FCCP), and 2 μM (for 3T3-L1) or 4 μM antimycin A (for C2C12) to determine OCRs due to proton leak, maximal, and non-mitochondrial respiration, respectively. $n = 4$ independent experiments, each independent experiment was done in five replicates. Data are presented relative to the vehicle as mean ± SEM. *, $p < 0.05$ and **, $p < 0.01$ compared with 0 nM (one-way ANOVA with Fisher's PLSD post hoc test). The exact mean and SEM values for data presented here can be found in Tables S8–S14. Note: ANOVA, analysis of variance; PLSD, protected least significant difference; SEM, standard error of the mean.

function in C2C12 myotubes (Figure 4E,F). As a control condition, we also exposed C2C12 myotubes directly to PCB126 for 24 h (Figure 4G,H). In contrast to our initial hypothesis, treatment of C2C12 myotubes with CM from IS or IR PCB126-treated adipocytes did not alter mitochondrial function (Figure 4E,F). Unexpectedly, control myotubes directly exposed to 100 nM PCB126 showed a significantly higher resting OCR, proton leak OCR, and maximal mitochondrial capacity compared with vehicle-treated cells (IS control myotubes: $p = 0.0037$ and 0.0302, for resting OCR and maximal capacity,

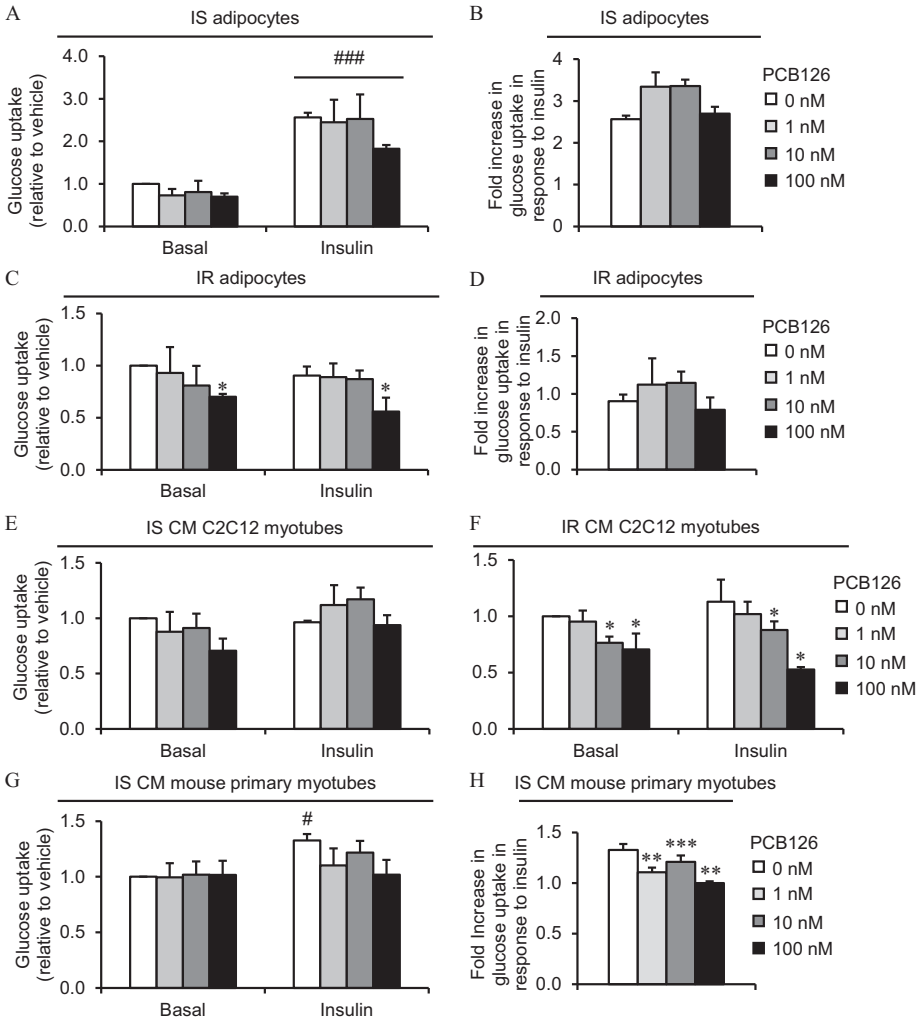

Figure 5. Glucose uptake in 3T3-L1 adipocytes exposed to PCB126 in different insulin sensitivity conditions and in C2C12 or mouse primary myotubes exposed to the conditioned medium (CM) of insulin sensitive (IS) and insulin resistant (IR) adipocytes treated with PCB126. (A–D) 3T3-L1 adipocytes were differentiated in IS (A,B) and IR (C,D) conditions and treated for the last 24 h of differentiation with different PCB126 concentrations. (A,C) Glucose uptake; (B,D) fold increase in glucose uptake in response to insulin. (E,F) Differentiated C2C12 myotubes were exposed for the last 24 h of differentiation to the CM of 3T3-L1 adipocytes exposed to different PCB126 concentrations in IS (E) or IR (F) conditions. (G,H) Differentiated mouse primary myotubes were exposed for the last 24 h of differentiation to the CM of 3T3-L1 adipocytes exposed to different PCB126 concentrations in IS conditions. (G) Glucose uptake; (H) fold increase in glucose uptake in response to insulin. (A–H) After differentiation and treatments, cells were subsequently treated ± 100 nM insulin for 20 min and exposed to 10 μM 2-deoxy-glucose and 0.5 μCi/mL ^{3}H-2-deoxy-glucose for 10 min. The absolute values of 2-deoxyglucose uptake under basal state (no insulin, no PCB126) were between 20 and 50 pmol/min/μg in 3T3-L1 adipocytes, between 50 and 80 pmol/min/μg in C2C12, and between 10 and 40 pmol/min/μg in mouse primary myotubes. Data are presented relative to the vehicle as mean $\pm$ SEM. $n = 3$–4 independent experiments, each independent experiment was done in three replicates. *, $p < 0.05$, **, $p < 0.01$, and ***, $p < 0.001$ compared with 0 nM; #, $p < 0.05$ compared with basal condition (no insulin) (for glucose uptake $\pm$insulin: two-way ANOVA with Fisher's PLSD post hoc test; for fold increase in response to insulin: one-way ANOVA with Fisher's PLSD post hoc test). The exact mean and SEM values for data presented here can be found in Tables S15–S19. Note: ANOVA, Analysis of variance; PLSD, protected least significant difference; SEM, standard error of the mean.

respectively; IR myotubes: $p = 0.0555$ and 0.0438, for resting and proton leak OCRs, respectively; Figure 4G,H).

Effect of Direct or Indirect PCB126 Exposure on Glucose Uptake in IS and IR Adipocytes and Myotubes

Glucose uptake in IS and IR adipocytes directly treated with PCB126. We then determined the effect of direct and indirect exposure to PCB126 on basal and insulin-stimulated glucose uptake in adipocytes and myotubes. Whereas adipocytes treated with insulin in IS conditions had significantly higher glucose uptake (Figure 5A), there was no significant difference in glucose uptake in response to insulin in IR adipocytes (Figure 5C). PCB126 exposure did not significantly alter basal or insulin-stimulated glucose uptake in IS adipocytes (Figure 5A and B), but IR adipocytes treated with 100 nM PCB126 had significantly lower glucose uptake in basal and insulin-stimulated conditions (PCB126 effect, $p = 0.0305$; Figure 5C and D). This difference in glucose uptake in IR adipocytes exposed to 100 nM PCB126 was not linked to any alteration in the phosphorylation of proteins of the insulin signaling pathway (p-IRS1, p-Akt, p-AS160; Figure S5A).

Glucose uptake in C2C12 myotubes directly treated with PCB126 or treated with the CM of PCB126-treated adipocytes. We then wanted to determine whether exposure to CM from 3T3-L1 adipocytes exposed to PCB126 altered glucose uptake in C2C12 myotubes (Figure 5E,F). As a control condition, we also exposed C2C12 myotubes directly to PCB126 for 24 h (Figure S6A). In control C2C12 myotubes, direct exposure to PCB126 did not significantly alter glucose uptake (Figure S6A). Exposure to

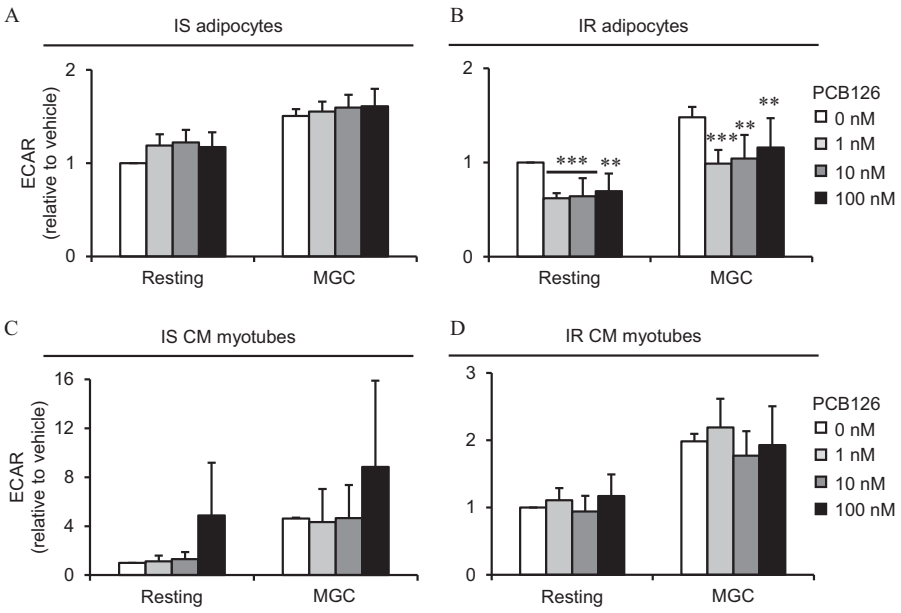

Figure 6. Glycolysis rates in 3T3-L1 adipocytes exposed to PCB126 in different insulin sensitivity conditions and in C2C12 exposed to the conditioned medium (CM) of insulin sensitive (IS) and insulin resistant (IR) adipocytes treated with PCB126. (A,B) 3T3-L1 adipocytes were differentiated in IS (A) and IR (B) conditions and treated for the last 24 h of differentiation with different PCB126 concentrations. (C–D) Differentiated C2C12 myotubes were exposed for the last 24 h of differentiation to the CM of 3T3-L1 adipocytes exposed to different PCB126 concentrations in IS (C) or IR conditions (D). Glycolysis rates were estimated by measuring extracellular acidification rates (ECAR) with a Seahorse analyzer (Agilent). ECAR were first measured in resting conditions, and cells were then treated with 600 ng/mL oligomycin to determine maximal glycolytic capacity (MGC). Data are presented relative to the vehicle as mean ± SEM. $n = 4$ independent experiments, each independent experiment was done in five replicates. *, $p < 0.05$, **, $p < 0.01$, and ***, $p < 0.001$ compared with 0 nM (one-way ANOVA with Fisher's PLSD post hoc test). The exact mean and SEM values for data presented here can be found in Tables S20–S23. Note: ANOVA, analysis of variance; PLSD, protected least significant difference; SEM, standard error of the mean.

CM from IS 3T3-L1 adipocytes (i.e., indirect PCB126 exposure) did not significantly alter glucose uptake in IS CM C2C12 myotubes in either basal or insulin conditions (Figure 5E). In contrast, C2C12 myotubes exposed to CM from IR 3T3-L1 adipocytes treated with 10 or 100 nM PCB126 had significantly lower glucose uptake in basal and insulin conditions compared with vehicle-treated cells ($p = 0.0349$ and $p = 0.0006$, respectively) (Figure 5F). As in IR adipocytes treated with PCB126, this lower glucose uptake in IR CM C2C12 myotubes was not linked to any alteration of the phosphorylation of proteins of the insulin signaling pathway (p-Akt, p-GSK3; Figure S5B).

Glucose uptake in mouse primary myotubes directly treated with PCB126 or treated with the CM of PCB126-treated adipocytes. It is recognized that insulin-stimulated glucose uptake is weak in C2C12 myotubes (Nedachi and Kanzaki 2006), and as expected, insulin treatment did not significantly increase glucose uptake in this model (Figure 5E and Figure S6A). Since one objective of the present study was to determine whether exposure to CM from PCB126-treated adipocytes altered insulin-stimulated glucose uptake in myotubes, we then used mouse primary myotubes, a muscle cell model more sensitive to insulin. Surprisingly, IS control myotubes directly exposed to 10 nM PCB126 tended to have a higher basal glucose uptake, without reaching significance ($p < 0.1$; Figure S6B). IR control myotubes treated with insulin did not have a higher glucose uptake compared with the basal condition, suggesting that the high insulin levels in IR conditions also induced insulin resistance in mouse primary muscle cells (Figure S6B). As a consequence, the effect of CM from IR adipocytes treated with PCB126 on insulin-stimulated glucose uptake in mouse primary myotubes could not be determined in IR conditions because the cells were already insulin resistant without PCB126 treatments. We then determined whether the CM from PCB126-treated adipocytes altered glucose uptake in mouse primary myotubes. A 24-h exposure to the CM from IS or IR adipocytes did not significantly alter basal glucose uptake in mouse primary myotubes compared with myotubes treated with the CM of vehicle-treated adipocytes (i.e., 0 nM PCB126) (Figure 5G and Figure S6C). However, the fold-differences in glucose uptake in response to insulin was less in mouse primary myotubes exposed to the CM of PCB126-treated IS 3T3-L1 adipocytes, suggesting insulin resistance development (1, 10, and 100 nM PCB126, $p < 0.01$; Figure 5H).

Effect of Direct or Indirect PCB126 Exposure on Glycolytic Rate in IS and IR Adipocytes and Myotubes

Glycolysis in IS and IR adipocytes directly treated with PCB126. To further study the effect of 24-h exposure to PCB126 on glucose metabolism, we next determined whether the impaired glucose uptake in IR adipocytes exposed to PCB126 could alter the glycolytic rate (Figure 6). In accordance with the glucose uptake results, a 24-h exposure to PCB126 did not alter the glycolytic rate in IS adipocytes (Figure 6A), but the resting glycolytic rate and maximal glycolytic capacity were significantly lower in IR adipocytes exposed to 1–100 nM PCB126 compared with the vehicle (for 1 nM, $p = 0.0008$ and 0.0007; for 10 nM, $p = 0.0012$ and 0.0018; and for 100 nM, $p = 0.0029$ and 0.0077, for resting and maximal glycolytic capacity, respectively) (Figure 6B).

Glycolysis in C2C12 myotubes directly treated with PCB126 or treated with the CM of PCB126-treated adipocytes. Myotubes exposed to CM from IS or IR adipocytes did not show any alteration in resting or maximal glycolytic rates (Figure 6C,D). Glycolytic rates in C2C12 myotubes were also not altered by direct exposure to the pollutant (Figure S7).

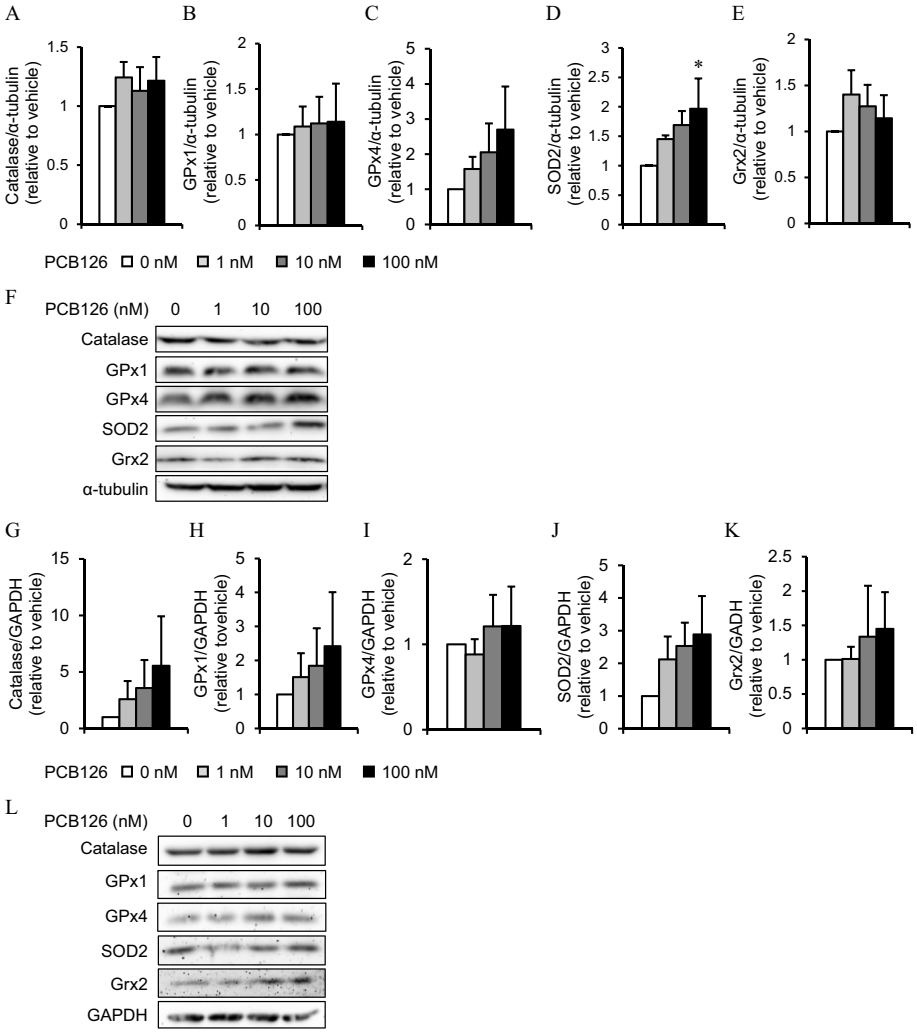

Figure 7. Oxidative stress markers in 3T3-L1 adipocytes exposed to PCB126 in insulin resistant (IR) conditions and in C2C12 myotubes exposed to the conditioned medium (CM) of PCB126-treated IR adipocytes. Levels of oxidative stress markers in (A–F) 3T3-L1 adipocytes differentiated in IR conditions and exposed for 24 h to different concentrations of PCB126 or (G–L) C2C12 myotubes exposed to the CM of PCB126-treated IR adipocytes. (A–E, G–K) Quantification by density analysis[catalase (A,G), glutathione peroxidase (GPx) 1 (B,H) and 4 (C,I), superoxide dismutase (SOD) 2 (D,J), glutaredoxin (Grx) 2 (E,K)], and (F,L) representative Western blots. (A–F) α-Tubulin and (G–L) GAPDH were used as loading controls. $n = 3$–6 independent experiments. Data are presented relative to the vehicle as mean ± SEM. *, $p < 0.05$ compared with 0 nM (one-way ANOVA with Fisher's PLSD post hoc test). The exact mean and SEM values for data presented here can be found in Tables S24 and S25. Note: ANOVA, analysis of variance; GAPDH, glyceraldehyde-3-phosphate dehydrogenase; PLSD, protected least significant difference; SEM, standard error of the mean.

Effect of Direct or Indirect PCB126 Exposure on Oxidative Stress Markers in IR Adipocytes and Myotubes

Expression of anti-oxidant enzymes in IR adipocytes directly treated with PCB126. To better determine whether oxidative stress may explain altered metabolism induced by PCB126 in IR conditions, we measured the levels of ROS detoxification enzymes in IR adipocytes after a 24-h exposure to PCB126. IR adipocytes treated with 100 nM PCB126 had a significantly higher expression of SOD2 ($p = 0.0288$), whereas other oxidative stress markers were not significantly different after PCB126 exposure (Figure 7A–F).

Oxidative stress markers in C2C12 myotubes treated with the CM of PCB126-treated IR adipocytes. In myotubes exposed to the CM of PCB126-treated IR adipocytes, the levels of catalase and SOD2 also tended to be higher compared with vehicle-treated cells, but it did not reach significance (Figure 7G,J,L). The levels of other ROS detoxification enzymes were not altered in myotubes exposed to the CM of PCB126-treated IR adipocytes (Figure 7H,I,K,L).

Effect of Direct or Indirect PCB126 Exposure on the Active Form of AMPK in IR Adipocytes and Myotubes

Expression of p-AMPK in IR adipocytes directly treated with PCB126. To determine whether AMPK, a key regulator of energy metabolism, was involved in the measured lower mitochondrial function and glucose uptake upon exposure to PCB126 in IR adipocytes, we measured the levels of the activated form of AMPK (i.e., p-AMPK). IR adipocytes exposed to 100 nM PCB126 had significantly lower levels of p-AMPK compared with vehicle-treated cells ($p = 0.0078$; Figure 8A,B).

Expression of p-AMPK in C2C12 myotubes treated with the CM of PCB126-treated IR adipocytes. We then determined whether the altered glucose uptake in C2C12 myotubes exposed to the CM of PCB126-treated IR adipocytes was also linked to lower AMPK activation. Curiously, in C2C12 myotubes exposed to the CM of PCB126-treated IR adipocytes, p-AMPK levels were significantly higher rather than lower compared with the vehicle ($p = 0.011$; Figure 8C,D).

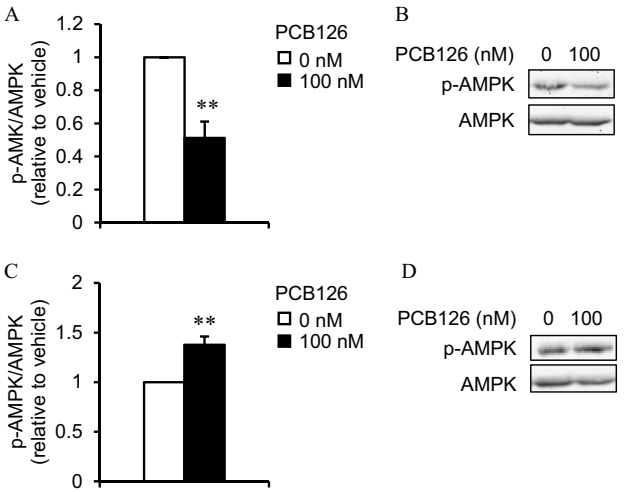

Figure 8. AMP-activated protein kinase (AMPK) levels in 3T3-L1 adipocytes exposed to PCB126 in insulin resistant (IR) conditions and in C2C12 myotubes exposed to the conditioned medium (CM) of PCB126-treated IR adipocytes. Levels of p-AMPK/AMPK in (A,B) 3T3-L1 adipocytes differentiated in IR conditions and exposed for 24 h to 100 nM of PCB126 or (C,D) C2C12 exposed to the CM of IR adipocytes exposed to 100 nM PCB126. (A,C) Quantification by density analysis; (B,D) representative Western blots. $n = 3$ independent experiments. Data are presented relative to the vehicle as mean ± SEM. **, $p \leq 0.01$ compared with 0 nM (Student's *t*-test). The exact mean and SEM values for data presented here can be found in Tables S26 and S27. Note: SEM, standard error of the mean.

Discussion

Exposure to PCB126 has been associated with the development of mitochondrial dysfunction in rat liver (Connell et al. 1999) and in rat skeletal muscle tissue (Tremblay-Laganière et al. 2019), with insulin resistance in 3T3-L1 adipocytes and *in vivo* in mice (Kim et al. 2017), and with decreased basal glucose uptake in L6 myotubes (Mauger et al. 2016). PCB126 is a lipophilic compound that has been shown to increase inflammation in human preadipocytes (Gadupudi et al. 2015; Gourronc et al. 2018), and increased adipose tissue inflammation is one potential cause of insulin resistance and mitochondrial dysfunction development in skeletal muscle, as nicely reviewed by Guilherme et al. (2008) and Saltiel and Olefsky (2017). The general objective of the present study was to determine the role of adipose-to-muscle communication in the development of mitochondrial dysfunction and glucose metabolism alterations in skeletal muscle when exposed to PCB126. Using an *in vitro* model, we showed that PCB126 altered the expression/secretion of adipokines and altered adipocyte mitochondrial function and glucose uptake, especially when adipocytes were rendered insulin resistant. These metabolic alterations were accompanied by higher SOD2 levels, which are known to be involved in ROS detoxification, and by lower activation of AMPK, an important metabolic sensor. Furthermore, myotubes exposed to the CM of IR adipocytes treated with PCB126 showed altered glucose uptake compared with myotubes exposed directly to PCB126. However, exposure of myotubes to the CM of PCB126-treated adipocytes did not alter their mitochondrial function but increased p-AMPK levels.

Effect of Preestablished Insulin Resistance on the Metabolic Response of Adipocytes to PCB126 Treatment

One objective of this study was to determine the effects of insulin resistance on the response of adipocytes to PCB126 exposure. Indeed, exposure to pollutants induced more significant metabolic defects in rodents developing obesity following a high-fat diet compared with their lean counterparts (Gray et al. 2013; Lim et al. 2009). For example, PCBs exacerbated hyperinsulinemia and insulin resistance in obese insulin resistant mice compared with lean insulin sensitive mice (Gray et al. 2013), suggesting increased sensitivity to pollutants when mice are already insulin resistant. Of note, in contrast to IS adipocytes, IR adipocytes exposed to PCB126 showed higher secretion of cytokines/adipokines, including TNF-α, IL-6, leptin, adiponectin, and MCP-1. These results suggested that preestablished insulin resistance in adipocytes made adipocytes more sensitive to the toxic effect of PCB126. This might be due to a better regulation of inflammatory response in metabolically healthy adipocytes. The present study focused on the effect of insulin sensitivity and PCB126 on pro-inflammatory cytokines, but how insulin resistance and PCB126 alter the secretion of anti-inflammatory cytokines such as IL-10 and IL-13 is also of interest and should be explored in future studies. Furthermore, it is important to note that, despite previous reports showing lower adiponectin mRNA levels and protein secretion in adipocytes exposed to coplanar PCBs (Arsenescu et al. 2008; Gadupudi et al. 2015), in the present study, adiponectin secretion was higher in IR adipocytes exposed to PCB126. The differences between our study and others can be due to a difference in the adipocyte model used (3T3-L1 vs. human adipocytes), in the concentration of coplanar PCB used (30–100 times lower in the present study), or the timing of PCB treatment (in previous studies, adipocytes were treated with coplanar PCBs during the whole differentiation process, whereas in the present study, adipocytes were treated for only 24 h, when the cells were already fully differentiated).

To the best of our knowledge, the effects of PCB126 exposure on glucose metabolism and mitochondrial function in adipocytes had never been studied. Therefore, the present study provides new insight into the role of PCB126 in adipose tissue metabolic dysfunction. The higher inflammation in IR adipocytes exposed to 100 nM PCB126 was associated with lower glucose uptake. Mitochondrial function and glycolysis were also lower in IR adipocytes exposed to PCB126 at concentrations of as low as 1 nM, and those results did not correspond to higher inflammation. Therefore, it seems that higher inflammation was probably not the cause of altered mitochondrial function and glycolysis in IR adipocytes. More studies are thus needed to better understand the mechanism by which PCB126 disrupts adipocyte energy metabolism. Importantly, exposure to PCB126 did not alter these metabolic pathways in IS adipocytes, showing that insulin sensitivity status might influence the response of adipocytes to PCB126 exposure.

The altered glucose metabolism and mitochondrial function in PCB126-treated IR adipocytes were associated with higher adipokine secretion and higher levels of SOD2. Interestingly, higher inflammation and oxidative stress are recognized as promoting mitochondrial dysfunction and altering glucose metabolism in adipocytes (Fazakerley et al. 2018; Manna and Jain 2015; Paglialunga et al. 2015; Steinberg 2007). In the present study, oxidative stress was estimated by measuring the levels of ROS detoxification enzymes. To better study the role of PCB126 in the development of oxidative stress in adipocytes, future studies should explore the impact of PCB126 on other important players in the modulation of oxidative stress, such as glutathione levels.

The negative effect of PCB126 on glucose metabolism and mitochondrial function in IR adipocytes was also associated with the lower activation of AMPK (i.e., its phosphorylation levels). AMPK is an important metabolic sensor known to activate glucose uptake independent of the insulin signaling pathway and to increase mitochondrial activity (Crawford et al. 2010; Jäger et al. 2007). Previously, a link between lower AMPK activation and

higher inflammation was demonstrated in 3T3-L1 adipocytes (Jung et al. 2018) and in the white adipose tissue of mice (Yang et al. 2016; Zhao et al. 2018). Our results therefore suggest that the lower glucose uptake and mitochondrial function in IR adipocytes exposed to 100 nM PCB126 might be the result of an alteration of the AMPK pathway because of higher inflammation/oxidative stress.

Role of Adipocyte-Secreted Factors in the Development of Muscle Cell Mitochondrial Dysfunction When Exposed to PCB126

Despite the role of skeletal muscle in the maintenance of glucose homeostasis, the effect of PCB126 or other environmental pollutants on skeletal muscle energy metabolism has not been well studied. High circulating levels of pollutants have been associated with decreased mitochondrial enzyme activity in human skeletal muscle (Imbeault et al. 2002). Furthermore, our team showed that PCB126 exposure in rats was associated with lower mitochondrial function in muscle (Tremblay-Laganière et al. 2019), which was not reproduced when muscle cells were directly exposed to the pollutant (Mauger et al. 2016). Here, we tested whether the adipose-to-muscle communication in the context of PCB126 exposure could induce mitochondrial dysfunction in skeletal muscle. However, CM from PCB126-treated IS or IR adipocytes did not alter mitochondrial function in C2C12 myotubes. Therefore, with the present model, we cannot confirm that the adipose-to-muscle communication was responsible for the decreased mitochondrial function in muscle from rats exposed to PCB126. Curiously, the activation of AMPK (i.e., p-AMPK levels) was higher rather than lower in C2C12 myotubes exposed to the CM of IR-treated adipocytes. Because AMPK is known to activate mitochondrial function, it is possible that C2C12 myotubes were able to maintain their mitochondrial function upon CM exposure because of increased AMPK activity.

Direct Effect of PCB126 on Glucose Metabolism in Muscle Cells

We have previously showed lower glycolytic function and glucose uptake in L6 myotubes exposed for 24 h to PCB126 (Mauger et al. 2016). Moreover, exposure to a PCB mixture (Aroclor 1254) has been shown to alter the skeletal muscle insulin signaling pathway and GLUT4 translocation in rats (Williams et al. 2013). In the present study, C2C12 or mouse primary myotubes directly exposed to the same concentrations of PCB126 as in our previous study using L6 myotubes (Mauger et al. 2016) showed no alteration of glucose uptake and glycolytic rates. These different effects of PCB126 on muscle cell glucose metabolism might be due to metabolic differences between L6, C2C12, and mouse primary myotubes. It is known that C2C12 mytotubes lack insulin-responsive GLUT4 vesicles required for significant insulin-stimulated glucose uptake (Tortorella and Pilch 2002), whereas L6 and primary mouse muscle cells possess these vesicles (Robinson et al. 1993; Tortorella and Pilch 2002). In addition, under conditions similar to ours (1 g/L glucose and 2% FBS), C2C12 myotubes expressed a greater proportion of slow myosin heavy chains (Artaza et al. 2002; Miller and Stockdale 1986; Miller 1990). Thus, C2C12 myotubes may have a more oxidative metabolism than L6 myotubes. This hypothesis has been confirmed in a recent study in which it was demonstrated that L6 cells had lower mitochondrial and fatty acid oxidation capacities than C2C12 cells while having higher emission of ROS (Robinson et al. 2019). Future studies should therefore determine whether the higher glycolytic capacity and higher ROS emission in L6 cells exposed to PCB126 may explain the fact that this muscle cell model was more sensitive to PCB126 than C2C12.

Role of Adipocyte-Secreted Factors in the Development of Altered Muscle Cell Glucose Uptake When Exposed to PCB126

Using the CM from PCB126-treated IR adipocytes, we showed that the adipocyte secretome decreased basal glucose uptake in C2C12 myotubes, whereas the CM from PCB126-treated IS adipocytes altered insulin sensitivity in mouse primary myotubes. Even if this altered glucose transport in myotubes was not associated with any alteration of the insulin signaling pathway, it is possible that GLUT4 content/translocation or GLUT1 levels/activity were affected. Further studies are thus needed to determine whether this altered glucose uptake was the result of an alteration of the expression or activity of GLUT1 or GLUT4.

One player in adipose-to-muscle communication is an altered secretion of fatty acids by adipose tissue (Rachek 2014), which might be promoted by PCB exposure (Regnier and Sargis 2014) or insulin resistance. However, in our model, the altered glucose uptake in myotubes exposed to the CM of PCB126-treated IS and IR adipocytes was probably not due to FFAs given that the lipolysis rate was lower rather than higher in IS adipocytes exposed to PCB126 and that the lipolysis rate was not altered in IR adipocytes exposed to PCB126.

Adipose tissue inflammation may be another player in the development of altered muscle glucose transport. Adipocytes secrete adipokines involved in autocrine/paracrine and endocrine functions. Adipokines alter metabolic responses locally in adipose tissue, as well as in distant tissues, such as skeletal muscle, as reviewed by Coles (2016), Luo and Liu (2016), and Scherer (2006). Under healthy conditions, adipokines maintain energy homeostasis, but dysregulation of adipokine secretion causes lipotoxicity in skeletal muscle (Coles 2016). In this sense, adipose tissue dysfunction has been associated with increased inflammation, which may explain the association between obesity and the increased risk of developing insulin resistance and type 2 diabetes. Of note, in the present study, PCB126 promoted inflammation in IR adipocytes in association with lower basal glucose uptake in myotubes exposed to IR adipocyte secretome. Similar results were obtained when muscle cells were treated directly with different adipocytokines, such as TNF-α, MCP-1, and IL-6 (Li et al. 2017; Sell et al. 2006). Taken together, the results from the present study and others suggest that PCB126-induced inflammation in adipose tissue might be responsible for the decreased insulin response and lower basal glucose uptake in muscle cells when exposed to PCB126 (Gadupudi et al. 2015; Gourronc et al. 2018; Williams et al. 2013). Interestingly, treatment with CM from hypoxia-treated 3T3-L1 adipocytes also induced insulin resistance in C2C12 myotubes (Yu et al. 2011), suggesting that different stressors might impact adipokine secretion, which in turn alters muscle insulin sensitivity. On the other hand, PCB126 treatment in IS adipocytes altered mRNA adiponectin expression but did not affect the secretion of adiponectin or other adipokines, suggesting that the effect of IS CM on myotube insulin sensitivity might be due to secreted factors other than the ones we measured in the present study. Further research is thus needed to determine which factor(s) secreted by PCB126-exposed IS adipocytes affected myotube insulin sensitivity. The potential candidates include adipocytokines not measured in our study (e.g., IL-1, IL-8, keratinocyte chemoattractant-1), metabolites that could be differentially secreted by adipocytes when exposed to PCB126, as well as micro-RNAs.

Limitations

Our conclusions are limited by our model, which studied a one-way communication between adipocytes and myotubes using cell

cultures *in vitro*. We acknowledge that this model does not fully represent what happens in an organism where the crosstalk between muscle and adipose tissue may also regulate metabolism (Bogdanowicz and Lu 2013; Li et al. 2017; Pandurangan et al. 2012). Our model was appropriate for our objectives in determining the role of PCB126 on adipokine secretion from adipocytes and how this altered muscle energy metabolism. However, it needs to be considered as an isolated system that possesses some limitations. Indeed, at the whole-body level, PCBs will also alter the secretion of cytokines and the production of ROS from other tissues and cell types, such as the liver, immune cells, and endothelial cells (Cocco et al. 2015; Lim et al. 2009; Tremblay-Laganière et al. 2019), which can then also alter muscle metabolism. Moreover, *in vivo*, PCBs might be metabolized by the liver, something that was not taken into account in our model. Last, our study focused on a PCB126 concentration (100 nM) that was higher than estimated environmental exposures, which may limit the generalization of our results. However, we studied the acute effect of a single pollutant (i.e., exposure for 24 h to PCB126), whereas humans are chronically exposed to several pollutants that may act in a similar fashion to PCB126. Further studies are thus required to determine whether exposure to a mix of pollutants for a longer period shows similar effects on adipose tissue metabolism and on adipose-to-muscle communication.

Conclusion

We have demonstrated that PCB126 promoted inflammation and metabolic defects in 3T3-L1 adipocytes in relation with decreased AMPK activity, particularly when those cells were already insulin resistant before exposing them to the pollutant. Moreover, our data suggest that the alteration of glucose uptake and the insulin response in skeletal muscle in response to PCB126 treatment was the result of PCB126-induced inflammation in adipose tissue. More broadly, our study shows the importance of the cross-talk between adipose tissue and skeletal muscle in the development of muscle insulin resistance.

Acknowledgments

Experiments were performed in C.A.'s laboratory at the Institut du Savoir Monfort (Ottawa, ON, Canada) and in E.A.'s laboratory at Health Canada (Ottawa, ON, Canada) except for the Seahorse and radiation experiments that were conducted in M.E. Harper's laboratory (Biochemistry, Microbiology, and Immunology Department, University of Ottawa, Canada). Conception and design of the experiments were done by C.A.; collection, assembly, analysis, and interpretation of data by A.C., F.A., V.P., L.G., E.A., and C.A.; drafting the article or revising it critically for important intellectual content by A.C., F.A., V.P., L.G., E.A., and C.A, and approval of the final version by A.C., F.A., V.P., L.G., E.A., and C.A.

The authors thank M.-E. Harper for the use of the XFe96 analyzer (Agilent) and the provision of her lab for radiation experiments, and M. Rigden for *Cyp1a1* mRNA determination. This work was funded by a Natural Sciences and Engineering Research Council of Canada (NSERC) Discovery Grant (2015–06263) to C.A. Master scholarships to A.C. were provided by the NSERC and Fonds de recherche du Québec – Santé and to L.G. by the Institut du Savoir Montfort.

References

Aguer C, Mercier J, Man CYW, Metz L, Bordenave S, Lambert K, et al. 2010. Intramyocellular lipid accumulation is associated with permanent relocation ex vivo and in vitro of fatty acid translocase (FAT)/CD36 in obese patients. Diabetologia 53(6):1151–1163, PMID: 20333349, https://doi.org/10.1007/s00125-010-1708-x.

Arsenescu V, Arsenescu RI, King V, Swanson H, Cassis LA. 2008. Polychlorinated biphenyl-77 induces adipocyte differentiation and proinflammatory adipokines and promotes obesity and atherosclerosis. Environ Health Perspect 116(6):761–768, PMID: 18560532, https://doi.org/10.1289/ehp.10554.

Artaza JN, Bhasin S, Mallidis C, Taylor W, Ma K, Gonzalez-Cadavid NF. 2002. Endogenous expression and localization of myostatin and its relation to myosin heavy chain distribution in C2C12 skeletal muscle cells. J Cell Physiol 190(2):170–179, PMID: 11807821, https://doi.org/10.1002/jcp.10044.

Baker NA, English V, Sunkara M, Morris AJ, Pearson KJ, Cassis LA. 2013. Resveratrol protects against polychlorinated biphenyl-mediated impairment of glucose homeostasis in adipocytes. J Nutr Biochem 24(12):2168–2174, PMID: 24231106, https://doi.org/10.1016/j.jnutbio.2013.08.009.

Beyer A, Biziuk M. 2009. Environmental fate and global distribution of polychlorinated biphenyls. Rev Environ Contam Toxicol 201:137–158, PMID: 19484591, https://doi.org/10.1007/978-1-4419-0032-6_5.

Bogdanowicz DR, Lu HH. 2013. Studying cell-cell communication in co-culture. Biotechnol J 8(4):395–396, PMID: 23554248, https://doi.org/10.1002/biot.201300054.

Bonnard C, Durand A, Peyrol S, Chanseaume E, Chauvin M-A, Morio B, et al. 2008. Mitochondrial dysfunction results from oxidative stress in the skeletal muscle of diet-induced insulin-resistant mice. J Clin Invest 118(2):789–800, PMID: 18188455, https://doi.org/10.1172/JCI32601.

Cocco S, Secondo A, Del Viscovo A, Procaccini C, Formisano L, Franco C, et al. 2015. Polychlorinated biphenyls induce mitochondrial dysfunction in SH-SY5Y neuroblastoma cells. PLoS One 10(6):e0129481, PMID: 26101884, https://doi.org/10.1371/journal.pone.0129481.

Coles CA. 2016. Adipokines in healthy skeletal muscle and metabolic disease. Adv Exp Med Biol 900:133–160, PMID: 27003399, https://doi.org/10.1007/978-3-319-27511-6_6.

Connell BJ, Singh A, Chu I. 1999. PCB congener 126-induced ultrastructural alterations in the rat liver: a stereological study. Toxicology 136(2–3):107–115, PMID: 10514003, https://doi.org/10.1016/S0300-483X(99)00062-1.

Crawford SA, Costford SR, Aguer C, Thomas SC, deKemp RA, DaSilva JN, et al. 2010. Naturally occurring R225W mutation of the gene encoding AMP-activated protein kinase (AMPK)γ_3 results in increased oxidative capacity and glucose uptake in human primary myotubes. Diabetologia 53(9):1986–1997, PMID: 20473479, https://doi.org/10.1007/s00125-010-1788-7.

Davis D, Safe S. 1990. Immunosuppressive activities of polychlorinated biphenyls in C57BL/6N mice: structure-activity relationships as Ah receptor agonists and partial antagonists. Toxicology 63(1):97–111, PMID: 2166363, https://doi.org/10.1016/0300-483X(90)90072-O.

EMD Millipore. 2013. Mouse bone magnetic bead panel. 96-well plate assay. Cat. No. MBNMAG-41K. Burlington, MA: EMD Millipore. https://filgen.jp/Product/Bioscience19-Bioplex/MBNMAG-41K_Protocol.pdf [accessed 15 September 2020].

Everett CJ, Frithsen IL, Diaz VA, Koopman RJ, Simpson WM Jr, Mainous AG III. 2007. Association of a polychlorinated dibenzo-*p*-dioxin, a polychlorinated biphenyl, and DDT with diabetes in the 1999–2002 National Health and Nutrition Examination Survey. Environ Res 103(3):413–418, PMID: 17187776, https://doi.org/10.1016/j.envres.2006.11.002.

Fazakerley DJ, Minard AY, Krycer JR, Thomas KC, Stöckli J, Harney DJ, et al. 2018. Mitochondrial oxidative stress causes insulin resistance without disrupting oxidative phosphorylation. J Biol Chem 293(19):7315–7328, PMID: 29599292, https://doi.org/10.1074/jbc.RA117.001254.

Ferrannini E, Smith JD, Cobelli C, Toffolo G, Pilo A, DeFronzo RA. 1985. Effect of insulin on the distribution and disposition of glucose in man. J Clin Invest 76(1):357–364, PMID: 3894421, https://doi.org/10.1172/JCI111969.

Gadupudi G, Gourronc FA, Ludewig G, Robertson LW, Klingelhutz AJ. 2015. PCB126 inhibits adipogenesis of human preadipocytes. Toxicol In Vitro 29(1):132–141, PMID: 25304490, https://doi.org/10.1016/j.tiv.2014.09.015.

Giesy JP, Kurunthachalam K. 2002. Dioxin-like and non-dioxin like effects of polyclorinated byphenyls: implications for risk assessment. Lakes Reservoirs: Res Manage 7(3):139–181, https://doi.org/10.1046/j.1440-1770.2002.00185.x.

Gourronc FA, Robertson LW, Klingelhutz AJ. 2018. A delayed proinflammatory response of human preadipocytes to PCB126 is dependent on the aryl hydrocarbon receptor. Environ Sci Pollut Res Int 25(17):16481–16492, PMID: 28699004, https://doi.org/10.1007/s11356-017-9676-z.

Gray SL, Shaw AC, Gagne AX, Chan HM. 2013. Chronic exposure to PCBs (Aroclor 1254) exacerbates obesity-induced insulin resistance and hyperinsulinemia in mice. J Toxicol Environ Health A 76(12):701–715, PMID: 23980837, https://doi.org/10.1080/15287394.2013.796503.

Guilherme A, Virbasius JV, Puri V, Czech MP. 2008. Adipocyte dysfunctions linking obesity to insulin resistance and type 2 diabetes. Nat Rev Mol Cell Biol 9(5):367–377, PMID: 18401346, https://doi.org/10.1038/nrm2391.

Imbeault P, Tremblay A, Simoneau J-A, Joanisse DR. 2002. Weight loss-induced rise in plasma pollutant is associated with reduced skeletal muscle oxidative

capacity. Am J Physiol Endocrinol Metab 282(3):E574–E579, PMID: 11832359, https://doi.org/10.1152/ajpendo.00394.2001.
International Diabetes Federation. 2020. Type 2 diabetes. Last updated 20 March 2020. https://www.idf.org/aboutdiabetes/type-2-diabetes.html [accessed 15 September 2020].
Jäger S, Handschin C, St.-Pierre J, Spiegelman BM. 2007. AMP-activated protein kinase (AMPK) action in skeletal muscle via direct phosphorylation of PGC-1α. Proc Natl Acad Sci USA 104(29):12017–12022, PMID: 17609368, https://doi.org/10.1073/pnas.0705070104.
Jung TW, Park HS, Choi GH, Kim D, Lee T. 2018. β-Aminoisobutyric acid attenuates LPS-induced inflammation and insulin resistance in adipocytes through AMPK-mediated pathway. J Biomed Sci 25(1):27, PMID: 29592806, https://doi.org/10.1186/s12929-018-0431-7.
Kim HY, Kwon WY, Kim YA, Oh YJ, Yoo SH, Lee MH, et al. 2017. Polychlorinated biphenyls exposure-induced insulin resistance is mediated by lipid droplet enlargement through Fsp27. Arch Toxicol 91(6):2353–2363, PMID: 27837308, https://doi.org/10.1007/s00204-016-1889-2.
Klip A, Li G, Logan WJ. 1984. Induction of sugar uptake response to insulin by serum depletion in fusing L6 myoblasts. Am J Physiol 247(3 pt 1):E291–E296, PMID: 6383069, https://doi.org/10.1152/ajpendo.1984.247.3.E291.
Kodavanti PRS, Ward TR, Derr-Yellin EC, Mundy WR, Casey AC, Bush B, et al. 1998. Congener-specific distribution of polychlorinated biphenyls in brain regions, blood, liver, and fat of adult rats following repeated exposure to Aroclor 1254. Toxicol Appl Pharmacol 153(2):199–210, PMID: 9878591, https://doi.org/10.1006/taap.1998.8534.
Krssak M, Falk Petersen K, Dresner A, DiPietro L, Vogel SM, Rothman DL, et al. 1999. Intramyocellular lipid concentrations are correlated with insulin sensitivity in humans: a 1H NMR spectroscopy study. Diabetologia 42(1):113–116, PMID: 10027589, https://doi.org/10.1007/s001250051123.
Li F, Li Y, Duan Y, Hu C-AA, Tang Y, Yin Y. 2017. Myokines and adipokines: involvement in the crosstalk between skeletal muscle and adipose tissue. Cytokine Growth Factor Rev 33:73–82, PMID: 27765498, https://doi.org/10.1016/j.cytogfr.2016.10.003.
Lim S, Ahn SY, Song IC, Chung MH, Jang HC, Park KS, et al. 2009. Chronic exposure to the herbicide, atrazine, causes mitochondrial dysfunction and insulin resistance. PLoS One 4(4):e5186, PMID: 19365547, https://doi.org/10.1371/journal.pone.0005186.
Longo M, Zatterale F, Naderi J, Parrillo L, Formisano P, Raciti GA, et al. 2019. Adipose tissue dysfunction as determinant of obesity-associated metabolic complications. Int J Mol Sci 20(9):2358, PMID: 31085992, https://doi.org/10.3390/ijms20092358.
Luo L, Liu M. 2016. Adipose tissue in control of metabolism. J Endocrinol 231(3):R77–R99, PMID: 27935822, https://doi.org/10.1530/JOE-16-0211.
Manna P, Jain SK. 2015. Obesity, oxidative stress, adipose tissue dysfunction, and the associated health risks: causes and therapeutic strategies. Metab Syndr Relat Disord 13(10):423–444, PMID: 26569333, https://doi.org/10.1089/met.2015.0095.
Matsuda M, Shimomura I. 2013. Increased oxidative stress in obesity: implications for metabolic syndrome, diabetes, hypertension, dyslipidemia, atherosclerosis, and cancer. Obes Res Clin Pract 7(5):e330–e341, PMID: 24455761, https://doi.org/10.1016/j.orcp.2013.05.004.
Matthews HB, Dedrick RL. 1984. Pharmacokinetics of PCBs. Annu Rev Pharmacol Toxicol 24(1):85–103, PMID: 6428301, https://doi.org/10.1146/annurev.pa.24.040184.000505.
Mauger J-F, Nadeau L, Caron A, Chapados NA, Aguer C. 2016. Polychlorinated biphenyl 126 exposure in L6 myotubes alters glucose metabolism: a pilot study. Environ Sci Pollut Res 23(8):8133–8140, PMID: 26936477, https://doi.org/10.1007/s11356-016-6348-3.
Miller JB. 1990. Myogenic programs of mouse muscle cell lines: expression of myosin heavy chain isoforms, MyoD1, and myogenin. J Cell Biol 111(3):1149–1159, PMID: 2167895, https://doi.org/10.1083/jcb.111.3.1149.
Miller JB, Stockdale FE. 1986. Developmental origins of skeletal muscle fibers: clonal analysis of myogenic cell lineages based on expression of fast and slow myosin heavy chains. Proc Natl Acad Sci USA 83(11):3860–3864, PMID: 3520558, https://doi.org/10.1073/pnas.83.11.3860.
Mogensen M, Sahlin K, Fernström M, Glintborg D, Vind BF, Beck-Nielsen H, et al. 2007. Mitochondrial respiration is decreased in skeletal muscle of patients with type 2 diabetes. Diabetes 56(6):1592–1599, PMID: 17351150, https://doi.org/10.2337/db06-0981.
Nedachi T, Kanzaki M. 2006. Regulation of glucose transporters by insulin and extracellular glucose in C2C12 myotubes. Am J Physiol Endocrinol Metab 291(4):E817–E828, PMID: 16735448, https://doi.org/10.1152/ajpendo.00194.2006.
Neel BA, Sargis RM. 2011. The paradox of progress: environmental disruption of metabolism and the diabetes epidemic. Diabetes 60(7):1838–1848, PMID: 21709279, https://doi.org/10.2337/db11-0153.
Paglialunga S, Ludzki A, Root-McCaig J, Holloway GP. 2015. In adipose tissue, increased mitochondrial emission of reactive oxygen species is important for short-term high-fat diet-induced insulin resistance in mice. Diabetologia 58(5):1071–1080, PMID: 25754553, https://doi.org/10.1007/s00125-015-3531-x.
Pandurangan M, Jeong D, Amna T, Van Ba H, Hwang I. 2012. Co-culture of C2C12 and 3T3-L1 preadipocyte cells alters the gene expression of calpains, caspases and heat shock proteins. In Vitro Cell Dev Biol Anim 48(9):577–582, PMID: 23054441, https://doi.org/10.1007/s11626-012-9550-8.
Perseghin G, Scifo P, De Cobelli F, Pagliato E, Battezzati A, Arcelloni C, et al. 1999. Intramyocellular triglyceride content is a determinant of in vivo insulin resistance in humans: a 1H-13C nuclear magnetic resonance spectroscopy assessment in offspring of type 2 diabetic parents. Diabetes 48(8):1600–1606, PMID: 10426379, https://doi.org/10.2337/diabetes.48.8.1600.
Pizzorno J. 2016. Is the diabetes epidemic primarily due to toxins? Integr Med (Encinitas) 15(4):8–17, PMID: 27574488.
Rachek LI. 2014. Free fatty acids and skeletal muscle insulin resistance. Prog Mol Biol Transl Sci 121:267–292, PMID: 24373240, https://doi.org/10.1016/B978-0-12-800101-1.00008-9.
Regnier SM, Sargis RM. 2014. Adipocytes under assault: environmental disruption of adipose physiology. Biochim Biophys Acta 1842(3):520–533, PMID: 23735214, https://doi.org/10.1016/j.bbadis.2013.05.028.
Robinson MM, Sather BK, Burney ER, Ehrlicher SE, Stierwalt HD, Franco MC, et al. 2019. Robust intrinsic differences in mitochondrial respiration and H_2O_2 emission between L6 and C2C12 cells. Am J Physiol Cell Physiol 317(2):C339–C347, PMID: 31091142, https://doi.org/10.1152/ajpcell.00343.2018.
Robinson R, Robinson LJ, James DE, Lawrence JC Jr. 1993. Glucose transport in L6 myoblasts overexpressing GLUT1 and GLUT4. J Biol Chem 268(29):22119–22126, PMID: 8408071.
Ruzzin J, Petersen R, Meugnier E, Madsen L, Lock E-J, Lillefosse H, et al. 2010. Persistent organic pollutant exposure leads to insulin resistance syndrome. Environ Health Perspect 118(4):465–471, PMID: 20064776, https://doi.org/10.1289/ehp.0901321.
Saltiel AR, Olefsky JM. 2017. Inflammatory mechanisms linking obesity and metabolic disease. J Clin Invest 127(1):1–4, PMID: 28045402, https://doi.org/10.1172/JCI92035.
Sargis RM. 2014. The hijacking of cellular signaling and the diabetes epidemic: mechanisms of environmental disruption of insulin action and glucose homeostasis. Diabetes Metab J 38(1):13–24, PMID: 24627823, https://doi.org/10.4093/dmj.2014.38.1.13.
Scherer PE. 2006. Adipose tissue: from lipid storage compartment to endocrine organ. Diabetes 55(6):1537–1545, PMID: 16731815, https://doi.org/10.2337/db06-0263.
Schmittgen TD, Livak KJ. 2008. Analyzing real-time PCR data by the comparative C_T method. 3(6):1101–1108, PMID: 18546601, https://doi.org/10.1038/nprot.2008.73.
Schneider CA, Rasband WS, Eliceiri KW. 2012. NIH Image to ImageJ: 25 years of image analysis. Nat Methods 9:671–675, https://doi.org/10.1038/nmeth.2089.
Sell H, Dietze-Schroeder D, Kaiser U, Eckel J. 2006. Monocyte chemotactic protein-1 is a potential player in the negative cross-talk between adipose tissue and skeletal muscle. Endocrinology 147(5):2458–2467, PMID: 16439461, https://doi.org/10.1210/en.2005-0969.
Singh K, Chan HM. 2017. Persistent organic pollutants and diabetes among Inuit in the Canadian Arctic. Environ Int 101:183–189, PMID: 28202225, https://doi.org/10.1016/j.envint.2017.02.002.
Steinberg GR. 2007. Inflammation in obesity is the common link between defects in fatty acid metabolism and insulin resistance. Cell Cycle 6(8):888–894, PMID: 17438370, https://doi.org/10.4161/cc.6.8.4135.
Tortorella LL, Pilch PF. 2002. C2C12 myocytes lack an insulin-responsive vesicular compartment despite dexamethasone-induced GLUT4 expression. Am J Physiol Endocrinol Metab 283(3):E514–E524, PMID: 12169445, https://doi.org/10.1152/ajpendo.00092.2002.
Tremblay-Laganière C, Garneau L, Mauger J-F, Peshdary V, Atlas E, Nikolla AS, et al. 2019. Polychlorinated biphenyl 126 exposure in rats alters skeletal muscle mitochondrial function. Environ Sci Pollut Res Int 26(3):2375–2386, PMID: 30467749, https://doi.org/10.1007/s11356-018-3738-8.
U.S. EPA (U.S. Environmental Protection Agency). 2003. 4. Human Exposures to CDD, CDF, and PCB Congeners. In: *Exposure and Human Health Reassessment of 2,3,7,8-Tetrachlorodibenzo-p-Dioxin (TCDD) and Related Compounds*. Part 1, Vol. 2. Washington, DC: U.S. EPA. https://cfpub.epa.gov/ncea/iris_drafts/dioxin/nas-review/pdfs/part1_vol2/dioxin_pt1_vol2_ch04_dec2003.pdf [accessed 15 September 2020].
Wang J, Lv X, Du Y. 2010. Inflammatory response and insulin signaling alteration induced by PCB77. J Environ Sci (China) 22(7):1086–1090, PMID: 21175000, https://doi.org/10.1016/S1001-0742(09)60221-7.
WHO (World Health Organization). 2010. Preventing disease through healthy environments. Exposure to dioxins and dioxin-like substances: a major public health concern. https://www.who.int/ipcs/features/dioxins.pdf?ua=1 [accessed 15 September 2020].
WHO. 2020. Diabetes 2020. Newsroom/Fact sheets. https://www.who.int/news-room/fact-sheets/detail/diabetes [accessed 15 September 2020].
Williams AA, Selvaraj J, Srinivasan C, Sathish S, Rajesh P, Balaji V, et al. 2013. Protective role of lycopene against Aroclor 1254-induced changes on GLUT4 in the skeletal muscles of adult male rat. Drug Chem Toxicol 36(3):320–328, PMID: 23035738, https://doi.org/10.3109/01480545.2012.720991.

Yang J, Leng J, Li J-J, Tang J-F, Li Y, Liu B-L, et al. 2016. Corosolic acid inhibits adipose tissue inflammation and ameliorates insulin resistance via AMPK activation in high-fat fed mice. Phytomedicine 23(2):181–190, PMID: 26926180, https://doi.org/10.1016/j.phymed.2015.12.018.

Yu J, Shi L, Wang H, Bilan PJ, Yao Z, Samaan MC, et al. 2011. Conditioned medium from hypoxia-treated adipocytes renders muscle cells insulin resistant. Eur J Cell Biol 90(12):1000–1015, PMID: 21962636, https://doi.org/10.1016/j.ejcb.2011.06.004.

Zhang S, Wu T, Chen M, Guo Z, Yang Z, Zuo Z, et al. 2015. Chronic exposure to Aroclor 1254 disrupts glucose homeostasis in male mice via inhibition of the insulin receptor signal pathway. Environ Sci Technol 49(16):10084–10092, PMID: 26190026, https://doi.org/10.1021/acs.est.5b01597.

Zhao P, Wong KI, Sun X, Reilly SM, Uhm M, Liao Z, et al. 2018. TBK1 at the crossroads of inflammation and energy homeostasis in adipose tissue. Cell 172(4):731–743.e12, PMID: 29425491, https://doi.org/10.1016/j.cell.2018.01.007.